Some Aspects of Microgrid Planning and Optimal Distribution Operation in the Presence of Electric Vehicles

by

Omar Hafez

A thesis
presented to the University of Waterloo
in fulfillment of the
thesis requirement for the degree of
Master of Applied Science
in
Electrical and Computer Engineering

Waterloo, Ontario, Canada, 2011

AUTHOR'S DECLARATION

I hereby declare that I am the sole author of this thesis. This is a true copy of the thesis, including any required final revisions, as accepted by my examiners.

I understand that my thesis may be made electronically available to the public.

Abstract

Increase in energy demand is one of the major challenges that utilities are faced with, thus resulting in an increase in environmental pollution and global warming. The transport sector has a significant share of the energy demand and is a major contribution of emissions to the environment. In Canada, almost 35% of the total energy demand is from the transport sector and it is the second largest source of greenhouse gas (GHG) emissions. The government of Ontario has aimed to move toward a green energy economy, thus resulting in increased penetration of renewable energy sources as well as Plug-in hybrid electric vehicle (PHEV) technology. Penetration of renewable energy sources into microgrids are gradually being recognized as important alternatives in supply side planning.

This thesis focuses on the optimal design, planning, sizing and operation of a hybrid, renewable energy based microgrid with the goal of minimizing the lifecycle cost, while taking into account environmental emissions. Four different configurations including a diesel-only, a fully renewable-based, a diesel-renewable mixed, and an external-grid connected microgrid are designed, to compare and evaluate their economics, operational performance and environmental emissions. Analysis is also carried out to determine the break-even economics for a grid-connected microgrid. The well-known energy modeling software for hybrid renewable energy systems, HOMER, is used in the studies reported in this thesis.

An optimal power flow (OPF) based optimization framework considering two different objectives, minimizing feeder losses and PHEV charging cost, are presented to understand the impact of PHEV charging on distribution networks. Three different charging periods are considered and the impact of the Ontario Time-of-Use (TOU) tariff on PHEV charging schedules is examined. The impact of PHEV charging on distribution systems in the presence of renewable energy sources is discussed by extending the developed OPF based model to include the contribution of renewable energy sources. The proposed model is evaluated under a variety of scenarios.

Acknowledgements

First and foremost, I would like to thank and praise Allah for helping me through this work and for providing me with all of my thesis great ideas, patience and health necessary for completion my Master degree.

Then, I also like to express my honest gratitude to my Professor Kankar Bhattacharya, for the continuous guidance, support, and encouragement he provided throughout the whole period of my master studies.

I would also like to thankful to Professor Jatin Nathwani and Professor Ramadan El-Shatshat for reading this thesis and providing their constructive comments and suggestions, that helped improve this work.

I gratefully appreciate the financial support from Saudi Cultural Bureau in Canada and my employer, Umm Alqura University.

Also I would thank all people in our labs for making these places as friendly places to work in I really enjoy it.

Many thanks also go to all technical and academic support provided by the Electrical and Computer Engineering Department at the University of Waterloo.

Finally, a heartfelt gratitude and indebted to my parents, my wife and my kids, for their true endless love and honest support inspired me to work hard and achieve what we are now proud of and for their patient and understanding even though it meant being away from them. I dedicate this thesis to my parents, my wife Alaa Hakeem, my daughter Lamar and my son Taha with love and appreciation.

Table of Contents

List of Figures

List of Tables

Chapter 1

Introduction

1.1 Motivation

The global demand for energy has been increasing rapidly, which imposes a great burden on existing energy resources, thus resulting in an exponential increase in environmental pollution and global warming. In the next 25 years, the global demand for energy is expected to increase by 50% because of the growth in population and economic development [1, 2].

Renewable energy resources are attracting the attention of energy developers. Renewable energy is also an important supply alternative for rural microgrids because of high oil prices and cost of transmission line expansion, combined with the desire to reduce carbon dioxide (CO_2) emissions. Although the cost of energy from conventional sources is typically lower than that from renewable energy sources, a supply-mix of renewable energy and diesel can reduce the overall cost of energy in a microgrid [3]. It is therefore important to examine the energy supply options in microgrids and determine the optimal supply mix, so that maximum benefits can be accrued from the design.

In Canada, the second highest source of greenhouse gas (GHG) emissions is the transportation sector, and it is one of the fastest growing contributors to energy demand. According to Transport Canada, almost 35% of the total energy demand in Canada is from the transport sector [4]. The awareness that significant global warming is being caused by vehicle emissions, is encouraging the transport sector to adopt plug-in hybrid electrical vehicles (PHEV) [6]. Renewable energy sources, combined with PHEV, presents significant benefits, but increased number of PHEVs can have a detrimental impact on the distribution system performance such as reduction in power quality, increase in power losses and voltage variations, as well as an adverse impact on the customers' energy price.

For distribution operators, meeting the increased demand arising from charging of the PHEVs while satisfying the distribution system operating constraints and reducing the system losses, is a major challenge. Moreover, as utilities establish the Time-of-Use (TOU)

tariffs and Smart Grid communication networks. There is a need to determine the optimal charging strategies that are beneficial to the distribution system and the PHEV customer.

1.2 Background

1.2.1 Microgrid

Around the world, governments and industries are moving towards use of cleaner energy sources and hence reduce the overall environmental pollution. This has led to an increase in attention towards Distributed Generation (DG) using non-conventional and renewable energy sources, which are connected locally at the distribution system level. However, adverse impact on the grid structure and its operation, with increased penetration of DGs, is unavoidable. To reduce the impact of DGs and make conventional grids more suitable for their large-scale deployment, the concept of microgrids is proposed [7].

A microgrid is an interconnection of DGs, either a set of dispatchable generating units such as, gas turbines and fuel cells or non-dispatchable generators such as, wind turbines and solar PV units, integrated with electrical and thermal energy storage devices to meet the customers' local energy needs, operating as a single system and small-scale, on low-voltage distribution systems providing both power and heat. To ensure that the microgrid is operated as a single aggregated system and meets power quality, reliability and security standards, power electronic interfaces and controls need to be applied [8-10]. This control flexibility allows the microgrid to present itself to the main utility power system as a single controlled unit.

The different modes of microgrid operation, i.e., microgrid connected to grid and stand-alone microgrid, are discussed in [11]. Stand-alone microgrids are typically designed for rural areas where supply from the main grid system is difficult because of the high costs of transmission line expansion. The associated benefits accrued are in reducing CO_2 emissions, feeder losses and providing local voltage support. In case of microgrids connected to the main grid, there are two options of connection- fully or partially connected. The connections are bidirectional, which means, the microgrid can export or import power to or

from the main grid. However, microgrids connected to the main grid can switch over to stand-alone mode if any fault occurs on the utility grid system.

The concept of microgrid is gaining rapid acceptance because of the environmentally friendly energy provision, its cost effectiveness, improvement in power quality and reliability, and reduction in line congestion and losses, reduction in infrastructure investment needs. From the customer point of view, the microgrid is designed to meet their electrical and heat energy demand and avoid load shedding [9].

1.2.2 Renewable Energy Resources

Canada, a world leader in the use of renewable energy, has vast renewable energy resources such as, moving water, biomass, wind, solar, geothermal and ocean energy because of its large landmass and diversified geography. In 2009, the contribution of renewable energy was about 16% of Canada's total primary energy supply [12]. Canada is also the second largest producer of hydroelectricity in the world, accounting for about 59% of the country's electricity generation, which is the most important renewable energy source in Canada [12]. With increasing concerns for global warming and environmental pollution, renewable energy has become an important alternative for the power sector. While wind and solar energy resources make smaller contributions as compared to hydro, in Canada, they have high penetration rates.

By the end of the year 2014, all coal-fired generation in Ontario is planned to be phase out, and the existing nuclear facilities are expected to reach their end of life [5]. Moreover, the Ontario Green Energy Act (GEA) proposes to reduce Ontario's impact on GHG emissions, as well as create significant employment in a green economy. According to [13], more than 28,000 MW of wind energy potential is available in Canada. By the year 2025, wind energy could be the supplier of 20% of Canada's electricity demand, as noted by Canadian Wind Energy Association (CanWEA) [14]. All these reasons lead Ontario to increasing the wind generation penetration in its electrical grid.

Investments in solar photovoltaic (PV) generation in Canada is increasing rapidly as compared to other regions of the world. Within the 2020-2030 time-frame lowest production cost, could be reached in Canada [15]. In [15] when replacing coal use by installed PV micropower, offset of 1.58 tonnes CO_2/year is reached.

1.2.3 PHEVs and Smart Charging

The electrical vehicle technology goes back to 1899, when Dr. Ferdinand Porsche and his team developed the first hybrid vehicle. In the late 1960s, when General Motors developed a vehicle that could be plugged into an electrical wall outlet, the PHEV concept was introduced. Since the turn of the 21st century, global warming, increase in gas price and poor air quality has become increasingly important issues that has driven the transport sector to move towards more fuel efficient vehicles. A best example of fuel efficient vehicle is the PHEV. There are three important categories of green vehicles as follows:

- Battery Electric Vehicle (BEV)- completely dependent on rechargeable battery. These vehicles have the capability to cut down overall emissions from the transport sector by 70% because no emission is produced by BEVs [17, 18].
- Hybrid Electric Vehicle (HEV)- combines internal combustion engine with an electric motor and battery. The battery is charged by utilizing energy from regenerative breaking and it reduces GHG smog by almost 90%.
- Plug-in Hybrid Electric Vehicle (PHEV)- uses gas and an external power outlet to charge its battery. The GHG emissions are reduced significantly and the overall efficiency of the energy conversion is high. PHEVs are a combination of the BEV and HEV because they run on battery for the first few miles and can switch over to hybrid mode [19].

The PHEV power train is classified into four different types as follows: series, parallel, series-parallel and complex hybrid configurations. [20].

The charging level of PHEV is classified into three types as specified by the National Electric Code (NEC) as well as in [21]. The three different charging levels are as follows:

- Level-1: Standard electrical outlet 120 V, single-phase, found in both residential and commercial buildings in Canada. The charging time is usually from 6 to 15 hours, depending on the size of the battery. The maximum power varies between 1.44 to 1.92 kW.
- Level-2: 240-V, single-phase ac supply, such outlets are found in many homes for electric cloth driers and electric ovens in Canada. The maximum power provided is limited to 7.2 kW because of the small charging system in the car which transfers the power from 120 V ac or 240 V ac outlets to dc voltages. The charging time is between 2 to 5 hours depending on the battery size.
- Level-3: 480-volt, three-phase supply which will allow very fast charging, and the system is still under development.

Smart charging platform communicates with the external grid using real-time, two-way communication technologies and connects directly with the grid, as shown in Fig-1.1 [22]. The U.S. Department of Energy (DoE) and Argonne National Laboratory (ANL) have developed an interactive technology in [22] for a smart charging platform that can inform the grid operator of the energy required to charge PHEVs, consumers' recharge preferences such as, time, cost threshold and billing information. The PHEV customers are provided with the consequences of charging at that time and the recommended time to charge, that would minimize cost as well as the impact on the grid and the environment.

Figure 1.1: Smart Charging platform developed by DOE and ANL [22]

1.3 Literature Review

Several studies have been reported to design optimal hybrid renewable-based microgrids for isolated systems, as discussed below.

Particle Swarm Optimization (PSO) technique is applied in [23] to determine the optimal number of PV modules installed, such that the total net economic benefit achieved over the system operational life, is maximized. Reference [24] reports the implementation of a wind-PV-diesel based hybrid microgrid system in three remote islands in Maldives. In [25], a feasibility analysis considering off-grid, stand-alone, renewable energy based microgrids for remote areas in Senegal demonstrate that the levelized electricity cost is lower than the

cost of energy from the grid expansions. In addition, the renewable energy based microgrid has a friendly impact on the environment.

In [26], the use of micro-hydro power is proven, and is favoured in remote area electrification needs instead of diesel generation, but it requires significant head. In [27], the authors develop an optimum sizing methodology to determine the dimensions of a hybrid energy supply system, while minimizing the capital cost. It is seen that the most attractive energy supply solution for the support of remote telecommunication stations is the proposed hybrid power system comprising PV, diesel, inverter and batteries.

In [28], a Mixed Integer Linear Programming (MILP) model is proposed for optimal planning of renewable energy systems for Peninsular Malaysia to meet a specified CO_2 emission reduction target. Mizani and Yazdani in [29], uses the HOMER software [30] to identify the optimal microgrid configuration and their optimal generation mix. The results show that optimal selection of renewable energy sources and energy storage devices in a grid-connected microgrid, in conjunction with an optimal dispatch strategy, can significantly reduce the lifetime cost and emissions of the microgrid.

The authors in [31], discuss ways to reduce fuel usage and hence minimize CO_2 emissions while maintaining a high degree of reliability and power quality for microgrids. This is achieved by maximizing the utilization of renewable resources, dispatching and scheduling the fossil fuel generators at their optimal efficiency operating points, by storing excess energy in a storage system, while reducing the dependency on the utility grid. A methodology for microgrid design and its economic feasibility with renewable energy sources is proposed in [32].

The economic operation of a combined heat and power (CHP) system consisting of wind power, PV, fuel cells, heat recovery boiler, and batteries is discussed in [33], using a non-linear optimization model. Forecasting of 24-hour wind speed, solar radiation, heat and electricity demand is considered as well. The optimal operation of a microgrid comprising wind power, PV, and battery, discussed in [34], uses a heuristic algorithm and linear model, and test results indicate that effective use of batteries can reduce the operating costs.

Off-grid electrification, by utilizing an Integrated Renewable Energy System (IRES), is proposed in [35] to satisfy the electrical and cooking needs of seven non-electrified villages in India. The National Renewable Energy Laboratory (NREL) provides information on hybrid renewable energy based microgrids, lessons learned from operational experience, and analysis of challenges and successes of the assessed systems [36]. A comparative analysis between diesel, hydro-diesel, and photovoltaic-diesel technologies is presented in [37] to analyze the field performance of different off-grid generation technologies applied to the electrification of rural villages in Jujuy, Argentina. The relevance of DGs and microgrids, in light of the emerging technologies, suitable for small islands in the Sundarbans, India is discussed in [38].

As we move toward a greener future, the PHEVs have an increasingly important role to play, because of their contribution to emissions reduction from the transportation sector. However, increased numbers of PHEVs can have a significant impact on the power distribution system performance. The study of the impact of electric vehicle charging profile goes back to the 1980s. Several studies show that the distribution grid can be significantly impacted by high penetration levels of PHEV charging. In [39, 40], the authors discuss that EV charging will likely coincide with overall system peak demand and thus, in order to avoid an overloading of the distribution feeders, adequate load management schemes should be in place. Furthermore, if there is no infrastructure to support EV charging at work, the increase in peak demand is much higher. In [41], it is suggested that the charging demand of EVs be controlled by a smart charging device to prevent charging during peak hours, otherwise the distribution feeders are overloaded.

In [42], three vehicle types, *i.e.*, battery, fuel cell and hybrid, that can produce vehicle-to-grid (V2G) power, and the electricity markets they can sell into is discussed. The author develops equations to evaluate revenue and costs for these vehicles to supply electricity to three electric markets (peak power, spinning reserves, and regulation). The author concludes that the proposed model increased stability and reliability of the electric grid, lower electric system costs. In [43], it is noted that PHEVs significantly increase demand side uncertainties, and potentially reduces the lifespan of the distribution feeder and

transformer. Even a 10% penetration of PHEV may cause unacceptable variations in the voltage profiles, if there is no regulation on PHEV charging [44]. In [45], the impact of EVs on a medium-voltage network as well as the Distribution System Operators' (DSO) benefits arising from use of smart charging schemes is discussed and determined. The paper notes that grid stability, need for infrastructure investment, and other challenges can be mitigated by adopting such smart charging strategies.

In [46], the impact of uncoordinated PHEV charging on system peak load, losses, and decrease in voltage and system load factor are discussed. In [47], the distribution networks in British Columbia, Canada are studied to determine the impact of uncoordinated PEV charging on the distribution voltage level using a probabilistic approach based on Monte Carlo simulations. In [48], it is shown that, applying the coordinated charging process can reduce system peak load, losses, and mitigate the impacts of uncoordinated PHEV charging in the distribution system. In [49], an optimization model is developed to determine the optimal and maximum penetration of PHEVs in the transport sector of Ontario considering the grid limitations.

From an environmental standpoint, many researchers have shown that PHEVs are environmentally friendly because they produce lower emissions as compared to conventional and hybrid electric vehicles [50]. In [51, 52], a multi-configurable eco-system consisting of a hybrid, wind and PV generation system with PHEVs, using data for Ohio, USA is developed to determine the energy and economic evaluation of PHEV and their interaction on grid and market. The impact of Time-of-Use (TOU) rates on charging of PHEVs and the effect of higher price during peak hours on shifting the EV load is discussed in [53].

Simultaneous charging of a large number of PHEVs and should ideally be carried out during lower price periods. In this thesis, the optimal charging profile of 1000 PHEVs in a charging station is considered, taking into account the different objectives, from the perspective of the DSO and the customer. Also the contribution of renewable energy sources is discussed in details and the Ontario TOU is used to evaluate its impact on charging PHEVs.

1.4 Objective of This Research

The main objectives of this thesis can be outlined as follows:

- Determine the optimal design of renewable energy based microgrids considering various renewable energy technology options and with realistic inputs on their physical, operating and economic characteristics.
- Determine the break-even distance for connection of the microgrid with the main grid and compare that with the cost of the isolated microgrid. Compare the overall benefits from the optimally designed renewable energy based microgrid with existing microgrid configurations.
- Develop a modeling framework for distribution system operations considering PHEVs to examine their impact on the feeder losses as well as voltage deviations. Determine the impact of PHEV charging on the customer costs, considering the Ontario TOU tariff structure.
- Incorporate renewable energy sources in the distribution system model with PHEV in order to examine their impact on the distribution system performance as well as how they will affect the PHEV charging profile.

1.5 Outline of this Thesis

This thesis is organized into five chapters as follows:

Chapter 1 presents the introduction and motivation for this research. Brief review of microgrids, renewable energy, and PHEV is presented and the objectives of this thesis are outlined.

Chapter 2 presents the optimal design and planning of a renewable energy based microgrid considering various renewable energy technology options and with realistic inputs on their physical, operating and economic characteristics. The break-even distance is determined for connection of the microgrid with the main grid, and compared with the cost of the isolated microgrid. Finally, the overall benefits from the optimally designed renewable energy based microgrid with existing microgrid configurations are compared.

Chapter 3 presents an OPF based optimization framework for operation of the distribution system. First, the optimal charging profiles of PHEVs under different scenarios are comprehensively discussed. The impact of the PHEV on the distribution system as well as on the PHEV customers cost is discussed in detail. Finally, the proposed optimization planning models are evaluated under a variety of scenarios.

Chapter 4 the impact of PHEV charging on the distribution system in the presence of renewable energy sources is discussed. In this chapter also, the OPF based model developed in chapter 3 is extended to include the contribution of renewable energy sources in order to determine the optimal charging periods of PHEVs and the impact of renewable energy sources.

Chapter 5 summarizes the conclusions and main contributions of this thesis and suggests directions for future research work.

Chapter 2

Optimal Planning and Design of a Renewable Energy Based Microgrid

2.1 Introduction

With the price of oil reaching its highest levels and the costs of transmission line expansion rapidly increasing, combined with the desire to reduce carbon dioxide emissions, renewable energy has become an important alternative as a power provider in rural systems. The cost of energy from conventional sources is less than that from renewable energy sources, but a supply-mix of renewable energy and diesel can reduce the cost of energy [54].

Energy demands are increasing rapidly, requiring energy resources to meet these demands, resulting in an exponential increase in environmental pollution and global warming. On the other hand, these days renewable energy, which is clean and limitless sources of energy, is catching the attention of energy developers. However, the estimation of the correct type of renewable energy system needs to be done under optimizations technique. In addition, for remote, rural isolated power systems, renewable energy sources are being increasingly recognized as cost-effective generation sources. In isolated areas, the high cost of transmission lines and higher transmission losses are encouraging the use of green sources of energy. Combining two or more renewable energy sources, such as solar, wind, hydro, diesel, etc., together gives a stable energy supply in comparison to non-renewable energy systems.

The planning of microgrid in rural areas, considering renewable energy sources, requires the definition of several factors, such as: the best sources of renewable energy to be used, the number and capacity of these generation sources, the total system cost, the amount of emissions that can be saved, the distance from the nearest grid connecting point, the excess energy, unmet load, diesel prices, different loads, and grid connected systems. In addition, in many countries governments strongly encourage the planners of microgrids to be motivated towards investment in the renewable energy sector. In this chapter, all of the above

factors, as well as their effect on the proposed system, are examined. The main objectives of this chapter can be outlined as follows:

- Optimal design and planning of a renewable energy based microgrid considering various renewable energy technology options and with realistic inputs on their physical, operating and economic characteristics.
- To determine the break-even distance for connection of the microgrid with the main grid, and compare that with the cost of the isolated microgrid.
- Compare the overall benefits from the optimally designed renewable energy based microgrid with existing microgrid configurations.

The rest of the chapter is organized as follows: Section-2.2 presents the problem definition, Section-2.3 briefly discusses the system under consideration and the system input data, Section-2.4 gives a brief description of the HOMER simulation tool and its capabilities, in Section-2.5 different study cases considering the optimal microgrid design is carried out and the results are presented and discussed, and finally in Section-2.6 presents the summary and conclusions of this chapter.

2.2 Problem Definition

The two principal economic elements, the total net present cost (NPC) and the levelized cost of energy (COE), depend on the total annualized cost of the system. To calculate the total net present cost the following equation is used:

$$C_{NPC} = \frac{C_{TANN}}{CRF_{(i,N)}} \tag{2.1}$$

Where C_{TANN} is the total annualized cost, i is the annual real interest rate (the discount rate), N is the number of years, $CRF_{(i,N)}$ is the capital recovery factor, and it is calculated as follows:

$$CRF_{i,N} = \frac{i(1+i)^N}{(1+i)^{N-1}} \tag{2.2}$$

In addition, the following equation is used to calculate the levelized COE:

$$\mathrm{COE} = \frac{\mathrm{C_{TANN}}}{\mathrm{E_{ls}} + \mathrm{E_{grid}}} \tag{2.3}$$

Where E_{ls} is the electrical energy that the microgrid system actually serves and E_{grid} is the amount of electricity sold to the grid by microgrid. In the levelized COE equation (2.3), the total annualized cost is divided by the electrical load that the microgrid actually serves, plus the amount of electricity sold to the grid by microgrid. In HOMER, the total NPC is the preferable objective function and has been used in the optimization process instead of the levelized COE [55].

2.3 System under Consideration

The available energy supply options in the hybrid microgrid system design under consideration comprises wind turbines, solar PV array, battery bank, hydro turbines, diesel generator, dump load, boiler and an AC/DC converter (Fig.2-1). The characteristics and cost of the system components are presented in the following sub-sections.

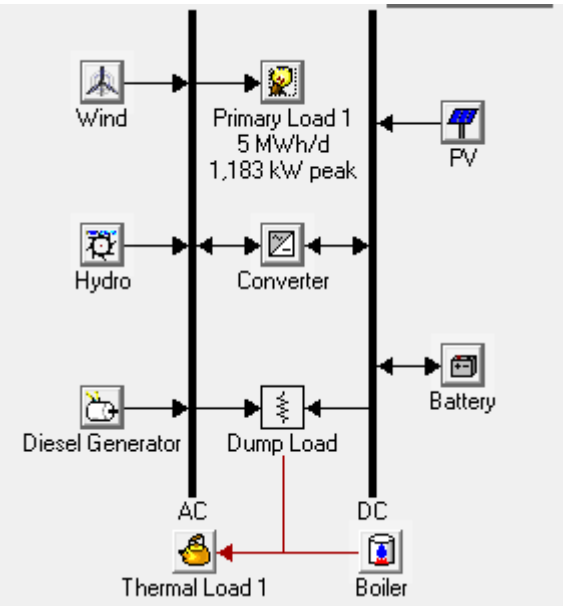

Figure 2-1: Available portfolio of energy supply options in microgrid planning

2.4 Assumptions and Model Inputs

2.4.1 AC Load

Figure 2-2 illustrates a typical daily load profile of the hypothetical rural community. The energy consumed by the microgrid is 5000 kWh/day with a 1183 kW peak demand.

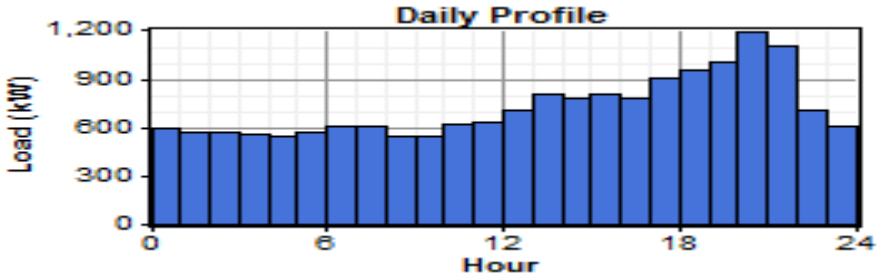

Figure 2-2: Hourly electrical load profile of microgrid

The data source is synthetic and 15% of daily noise and 20% of hourly noise is considered. The mechanism for adding daily and hourly noise is simple: HOMER randomly draws the daily perturbation factor once per day *f*rom a normal distribution with a mean of zero and a standard deviation equal to the daily noise input value. In addition, it randomly draws the hourly perturbation factor every hour from a normal distribution with a mean of zero and a standard deviation equal to the hourly noise input value [30]. The scaled annual averages are 1000, 3000, and 5000 kWh/d. The scaled peak loads are 237, 710, and 1138 kW, with a load factor of 0.176.

2.4.2 Thermal Load

In this chapter the thermal load is assumed to be only 5% of the primary load (Figure 2-3). The scaled annual average is 500 kWh/d. The scaled peak load is 51.07 kW, with a load factor of 0.355. The idea of adding thermal load in this chapter is to examine the impact of excess energy feeding thermal load.

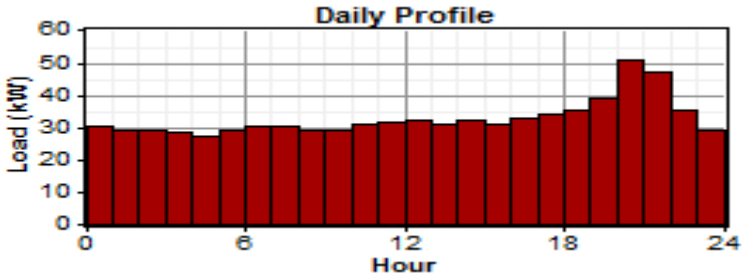

Figure 2-3: Hourly electrical load profile of microgrid

2.4.3 Solar Resource

The solar radiation profile of Waterloo, Ontario, (43° 39' N, 80° 32' W) is considered for this work. Solar radiation data is obtained from the NASA Surface Meteorology and Solar Energy website [56]. The annual average solar radiation for this area is 3.64 kWh/m^2/day. Figure 2-4 shows the month-wise average solar radiation profile over a one-year period.

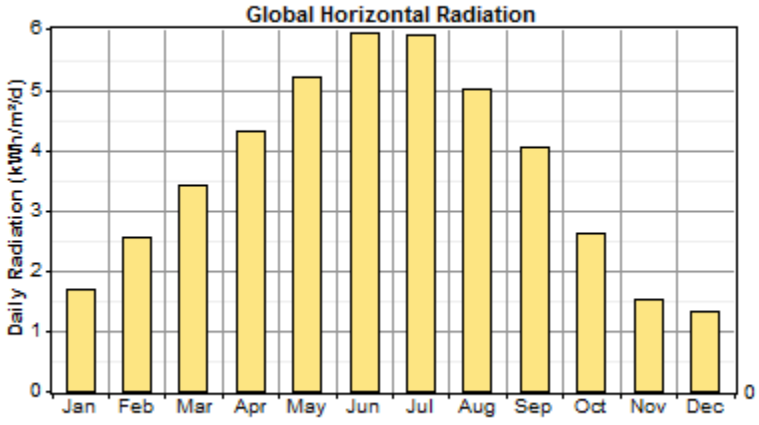

Figure 2-4: Solar radiation profile for Waterloo

2.4.4 Photovoltaic Panels

Photovoltaic panels' capital and replacement costs include shipping, tariffs, installation, and dealer mark-ups. Some maintenance is typically required on the PV panels. The derating

factor of 90% reduces the PV production by 10% to approximate the varying effects of temperature and dust on the panels.

2.4.5 Wind Resource

The wind speed profile of Waterloo, Ontario, (43° 39' N, 80° 32' W) is considered for this work. Wind data for this region is obtained from the Canadian Wind Energy Atlas [57]. The annual average wind for this area is 5.78 m/s. Figure 2-5 shows the month-wise average wind speed profile over a one-year period.

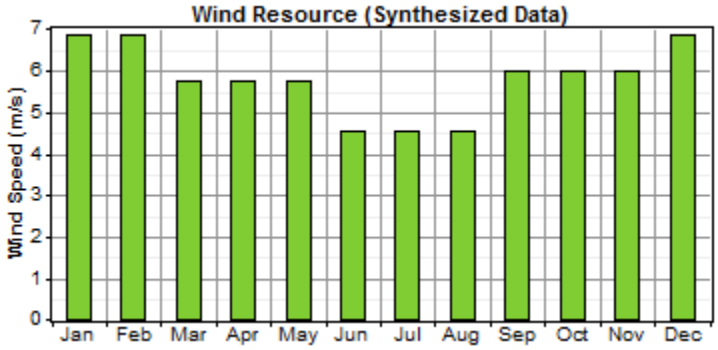

Figure 2-5: Wind speed profile for Waterloo

2.4.6 Wind Turbines

Wind turbine capital cost and replacement costs include shipping, tariffs, installation, and dealer mark-ups. The hub height is assumed to be 15m.

Table 2-1: Input Data on Option Costs

Options	Capital Cost	Replacement Cost	O&M Cost
Wind	$7900/turbine	$9000/turbine	$30/year
Solar	$7.50/W	$7.50/W	0
Micro-Hydro	$3600	$3600	$18/yr
Battery	$75/ Battery	$75/ Battery	$2/Battery /year
Converter	$1000/kW	$1000/kW	$100/year
Grid Extension	$20.000/km	$20.000/km	$10/year/km
Diesel Generator	For a 4.25 kW $2550	$2550	$0.15/h

Table 2-2: Input Data on Option Sizing and Other Parameters

Options	Options on Size and Unit Numbers	Life	Other Information
Wind	10, 50, 100, 500, 1000 turbines	15 yrs	Weibull distribution with *k=1.83*
Solar	1, 10, 100, 1000, 3000 kW	20 yrs	De-rating factor = 90%
Micro-Hydro	500 L/s flow rate	25 yrs	Scaled annual avg= 50, 100, 150 L/s
Battery	1, 1000, 5000, 10,000, 15,000, 20,000	845 kWh	Nominal capacity 225 Ah
Converter	0,1,10,50, 100, 500,1000 and 2000 kW	15 yrs	Can parallel with an AC generator. Converter Efficiency = 90% Rectifier Efficiency = 85%
Grid extension	-	-	Price of Electricity = $0.14/kWh
Diesel Generator	0 to 1,500 kW	5000 h	Minimum load ratio = 30%

2.4.7 Diesel Fuel Price

The study included a sensitivity analysis on the price of diesel fuel. This price can vary considerably based on region, transportation costs, and current market price. Prices of $0.30/L to $0.70/L are considered in this work, with a density of 820 kg/m, carbon content of 88%, and a sulfur content of 0.33%.

2.4.8 Economics

The annual real interest rate to be considered is 0.6%. The real interest rate is equal to the nominal interest rate minus the inflation rate. The project lifetime is 25 years.

2.4.9 Constraints

The constraints that must be added to the system are the maximum annual capacity shortage, varying from 0% to 10%. The minimum renewable fraction is set to 0%. The operating reserve is set as a percentage of the hourly load to 10%, the operating reserve as a percentage of the peak load to 0%, the operating reserve as a percentage of solar power output to 50%, and the operating reserve as a percentage of wind power output to 50%.

2.5 Hybrid Optimization Model for Electric Renewable (HOMER) Model

HOMER is a simulation tool developed by the U.S. National Renewable Energy Laboratory (NREL) to assist in the planning and design of renewable energy based microgrids. The physical behaviour of an energy supply system and its lifecycle cost, which is the sum of capital and operating costs over its lifespan, is modeled using HOMER [55]. Options such as stand-alone DG, off-grid and grid-connected supply systems for remote areas, and other design options, can also be evaluated using HOMER [30]. HOMER is designed to overcome the challenges of analysis and design of microgrids, arising from the large number of options and the uncertainty in key parameters, such as load growth and future fuel prices. Simulation, optimization, and sensitivity analysis are the three principal tasks performed in HOMER [55].

2.5.1 Simulation Module

In the simulation module, HOMER determines technical feasibility and life-cycle costs of a microgrid for each hour of the year. In addition, the microgrid configuration and the operation strategy of the supply components under the user-sizing definition are tested to examine how those components work together and would behave in a given setting over a long period of time [55].

2.5.2 Optimization Module

In the optimization module, HOMER displays the feasible systems with their configurations within the search space defined by the user, sorted by the least total NPC of the system. After the simulation module determines the system configuration of a microgrid, the optimization module determines the optimal system designs [55].

2.5.3 Sensitivity Analysis Module

In this module, the modeler can analyze the effects of parameter variations with time. The sensitivity variables are those variables which are entered by the user and have different values. The main objective of using the sensitivity analysis in HOMER is that if the user isn't sure which is the best value of a particular variable, then the user will enter different values and the sensitivity analysis will show how the results behave dependent on these values. Many optimizations have to be performed in this module by HOMER, each using different values of input assumptions [55].

2.6 Results and Discussions

In this section, four different cases are constructed in order to determine the most favorable option for microgrid planning as given in Table 2-3. In Case-1, the microgrid is assumed to be already in place, and is being supplied by an isolated network fed by diesel generators, as in the case of many remote power systems around the world that are dependent on imported fossil fuel to feed their demand. However, these units are very expensive because of their high cost of maintenance, fuel supply and fuel transportation. In addition, the diesel generators are highly emission intensive. Case-2 considers that the microgrid is entirely based on renewable energy sources, Case-3 is a mixed configuration comprising both diesel and renewable energy sources, while in Case-4 it is assumed that the microgrid has the option of connecting and drawing energy from the external grid.

Table 2-3: Summary of cases studied

Case	Description of Case
1	Diesel Dependent Microgrid (Base Case)
2	Renewable Based Microgrid (*wind, solar PV, battery, micro-hydro, converter*)
3	Diesel-Renewable Mixed Microgrid (*diesel, wind, solar PV, battery, micro-hydro, converter*)
4	Microgrid Connected to External Grid

2.6.1 Comparison of Various Cases

2.6.1.1 Optimal Plan Configurations and Cost Components

The optimal microgrid designs for the various cases considered are obtained from HOMER simulations, using the parameters as described in Section-2.3. The optimal microgrid configurations for the four cases are shown in Figure 2-6 (a)-(d). The corresponding details of the optimal microgrid plans for each case are presented in Table 2-4.

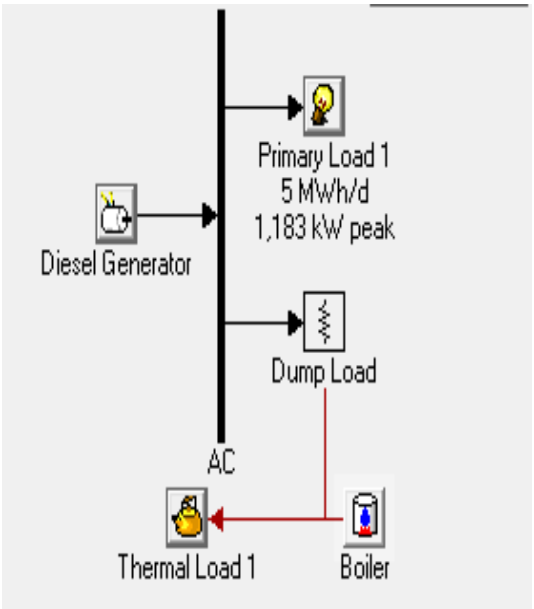

(a) Case-1

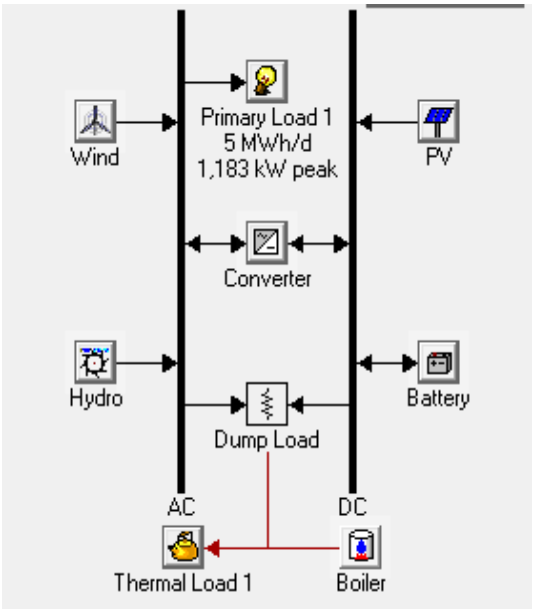

(b) **Case-2**

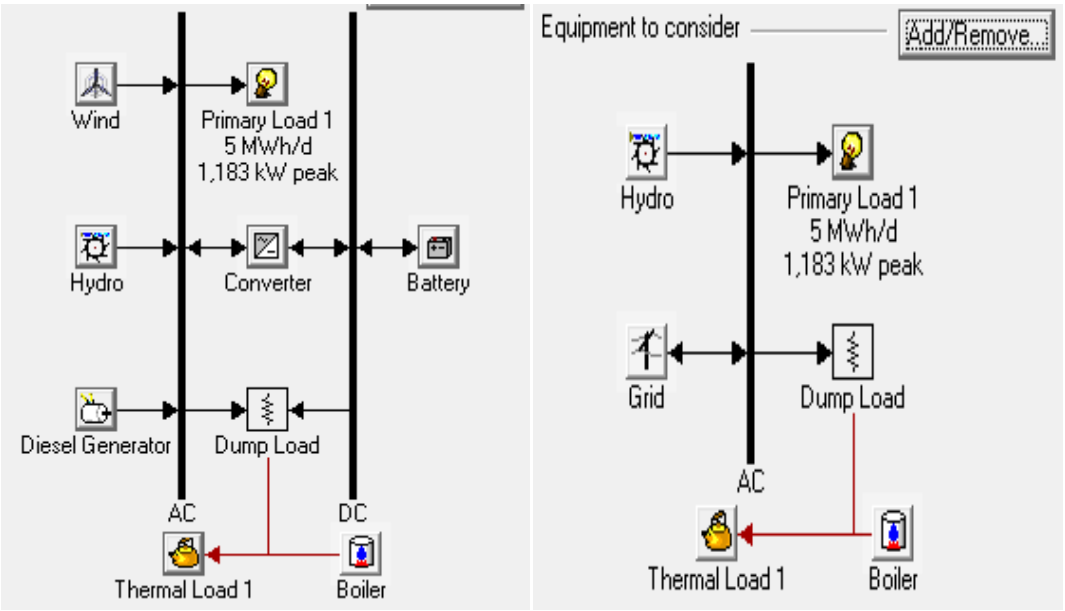

(c) Case-3 (d) **Case-4**

Figure 2-6: Comparison of Various Optimal Microgrid Configurations

Table 2-4: Optimal Microgrid Plan Configuration for Various Cases

Component	Case-1	Case-2	Case-3	Case-4
Diesel, kW	6,375	0	4,250	0
Solar PV, kW	0	500	0	0
Wind, kW	0	5000	1000	0
Converter, kW	0	1000	500	0
Battery, numbers	0	20,000	10,000	0
Micro-Hydro, kW	0	92	92	92
External Grid, kW	0	0	0	1,200

Table 2-5: Comparison of cost components for various cases

Items	Case-1	Case-2	Case-3	Case-4
Net Present Cost, M$	21.044	14.917	6.486	1.661
Levelized cost of energy, $/kWh	0.902	0.639	0.278	0.071
Operating Cost, M$/year	1.646	0.398	0.347	0.130

As stated earlier, this work is aimed at finding the least-cost microgrid plan while taking into account the environmental impact of each plan obtained from various cases considered. From the optimal microgrid configuration obtained, as presented in Figure 2-6

and Table 2-4, it is seen that while the diesel dependent microgrid (Case-1) selects 6,375 kW of diesel capacity to meet its demand, the renewable based microgrid (Case-2) completely relies on solar PV, wind, battery storage and micro-hydro generation. The diesel-renewable mixed microgrid (Case-3) opts for a reduced diesel generation capacity of 4,250 kW and some renewable capacity. Finally, it is noted that when the microgrid has an option of drawing energy from the external grid (Case-4), it relies on that option to a large extent. From Table 2-5 it is observed that the diesel-renewable mixed microgrid (Case-3) is the most economical option when external grid connectivity is not available. However, as many rural systems are fed through local generation, it is possible that some microgrid may connect to the external grid (Case-4) due to its reliability and that would be the cheapest option. However, if there is a need for the extension of the grid then, the NPC of Case-4 can be higher than any of the other cases depending on the connectivity distance of the microgrid. This will be discussed in Section 2.6.2.3.

It is also noted that the levelized cost of energy is significantly high in Case-1. Although in the renewable based microgrid (Case-2) the levelized cost is reduced somewhat, to 0.639 $/kWh, it is higher than the diesel-renewable mixed microgrid (Case-3) because of the significantly large capital cost component in the former, as shown in Figurers 2-7, 2-8. It is seen that the largest cost components in Case-1 are those of replacement, operation & maintenance and fuel costs while the capital cost is zero because the system was assumed to be in place, already. The largest cost components in Case-2 are capital and replacement costs while it is noted that the operation and fuel costs are very low. In Case-3 capital, replacement, operation & maintenance and fuel costs components are equally significant as shown in Figure 2-9, because of the mix of diesel with renewable sources, but they are much lower than the previous cases. In Case-4, as presented in Figure 2-10, the only cost component is the operation & maintenance cost which is essentially the cost of purchasing power from the grid.

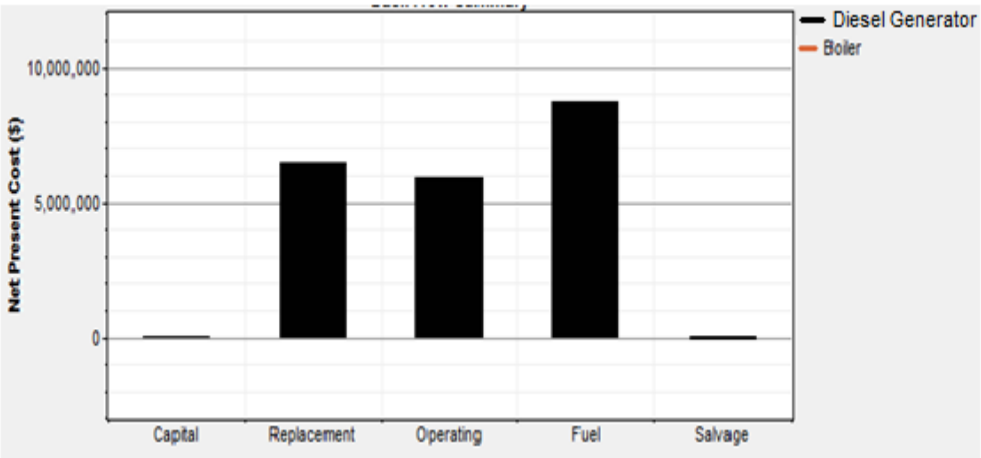

Figure 2-7: Cost components for Case-1 microgrid

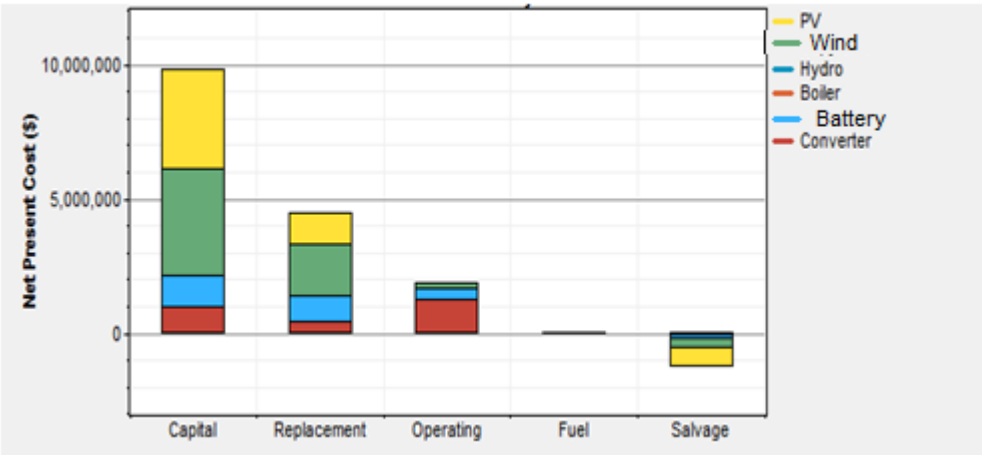

Figure 2-8: Cost components for Case-2 microgrid

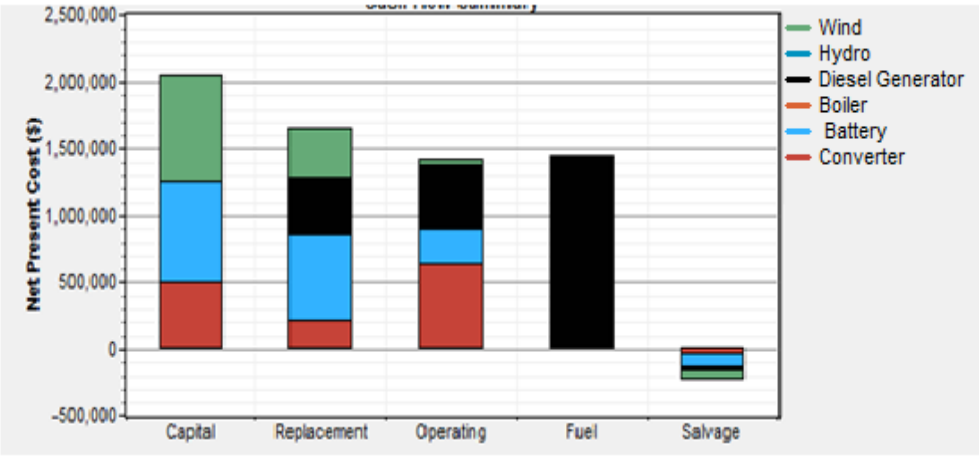

Figure 2-9: Cost components for Case-3 microgrid

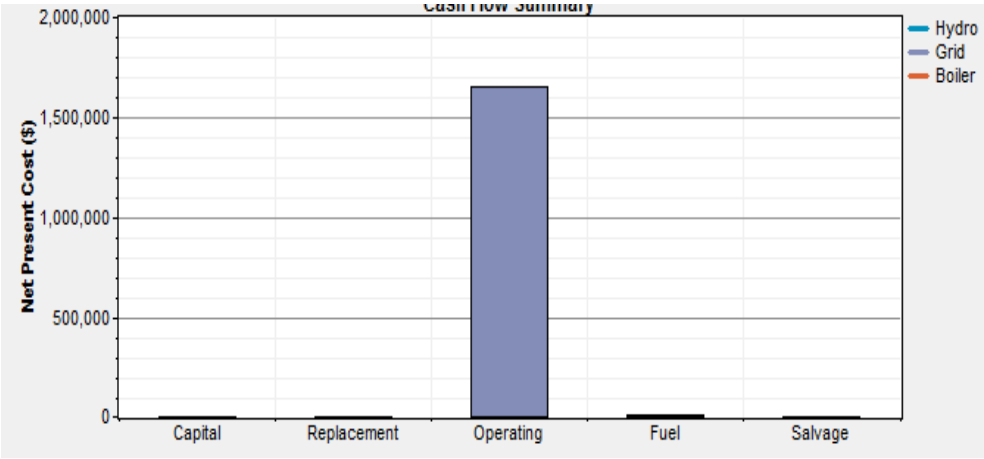

Figure 2-10: Cost components for Case-4 microgrid

Figure (2-11-2-13) presents the annual cash flows for the all cases, respectively. It is seen that in Case-1, the diesel generators incur a replacement cost every two years because of their operating life of 5000 h. Additionally, the system incurs a regular stream of cost of fuel and operation & maintenance. On the other hand, the renewable microgrid in Case-2 only incurs an initial investment cost while the replacement cost is sporadically distributed over its lifetime. In Case-3, the cash flow pattern is similar to Case-2, with an additional regular stream accounting for operation & maintenance cost arising because of the presence of diesel generator.

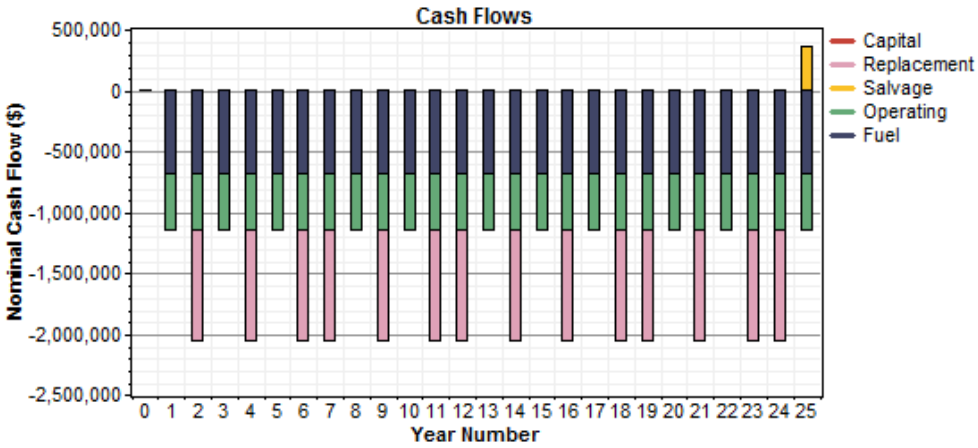

Figure 2-11: Cash flow in Case-1 microgrid

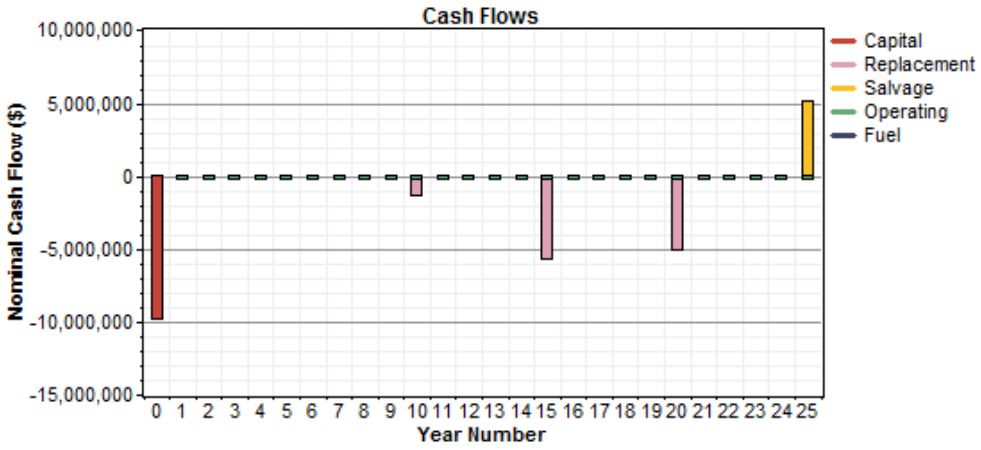

Figure 2-12: Cash flow in Case-2 microgrid

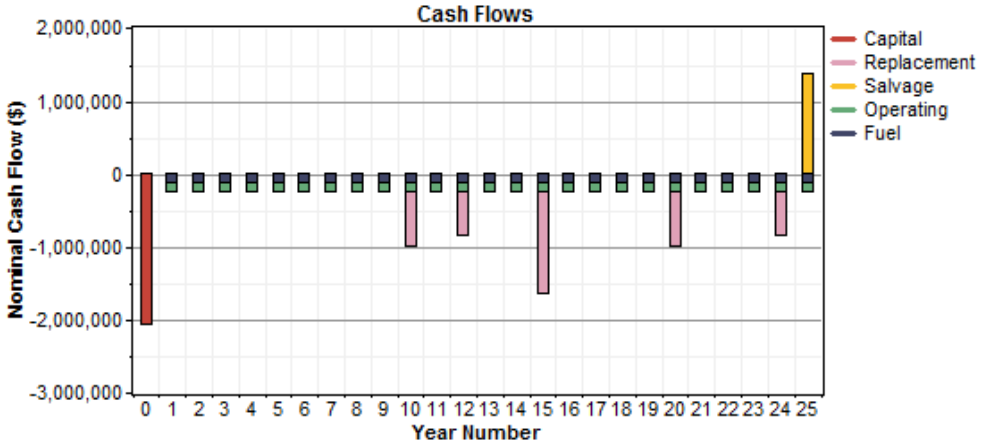

Figure 2-13: Cash flow in Case-3 microgrid

2.6.1.2 Optimal Production Profiles in Various Microgrid Configurations

Comparisons of electrical energy production and consumption for various microgrid configurations are conducted and presented in Table 2-6 and Figures (2-14-2-17). As shown in Table 2-6, in the renewable based microgrid (Case-2), the total energy produced is much higher than other cases, but still there is small unmet load, while the microgrid has to dump a substantial portion of the generation energy. This is because, renewable sources are intermittent and non-dispatchable and the microgrid being fully reliant on these sources in Case-2, is exposed to these risks. It is observed that although there is enough capacity, this

microgrid is not able serve the peak load at a few instances and thus the presence of energy, while it has to dump energy at some hours when the load is less. In Case-3 the excess energy is significantly reduced as compared to Case-2, because of the diesel and renewable energy mix, which results in a much lower microgrid capacity and better utilization of the generation. In Case-4 the excess energy is negative which means that the microgrid has to supply the thermal load from boilers because this microgrid essentially relies on external grid for serving its electrical load.

Table 2-6: Case-wise comparison of production and consumption

	Production, MWh/yr			
Component	**Case-1**	**Case-2**	**Case-3**	**Case-4**
Diesel Generator	4,101.52 (100%)	0	1,107.04 (46%)	0
Solar PV	0	633.5 (9%)	0	0
Wind	0	5,962.4 (89%)	1,192.48 (49%)	0
Micro-Hydro	0	115 (2%)	115 (5%)	115 (6%)
External Grid	0	0	0	1,710.25 (94%)
Renewable Energy Contribution	0%	100%	53.8%	6.25%
Total	4,101.52	6,710.84	2,414.51	1,825.25
	Consumption, MWh/yr			
Electrical Load Energy Served	1,825	1,824.87	1,825	1,825
Thermal Load Energy Served	182.5	182.5	182.5	182.5
Excess Energy to dump load	2094.02	4703.34	407.01	- 182.25
Unmet Energy	0	0.128	0	0

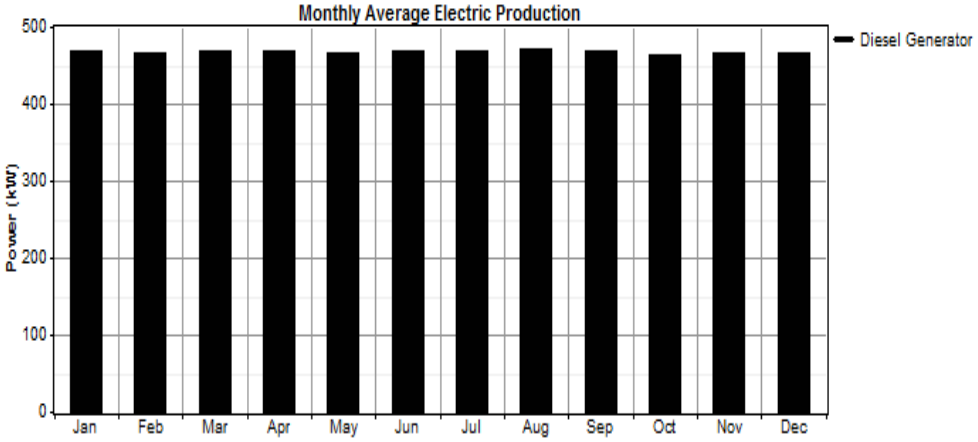

Figure 2-14: Power production in Case-1 Microgrid

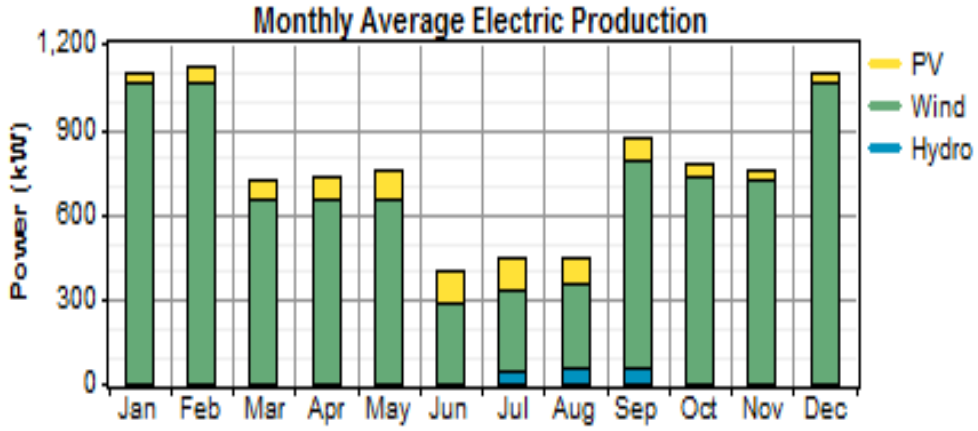

Figure 2-15: Power production in Case-2 Microgrid

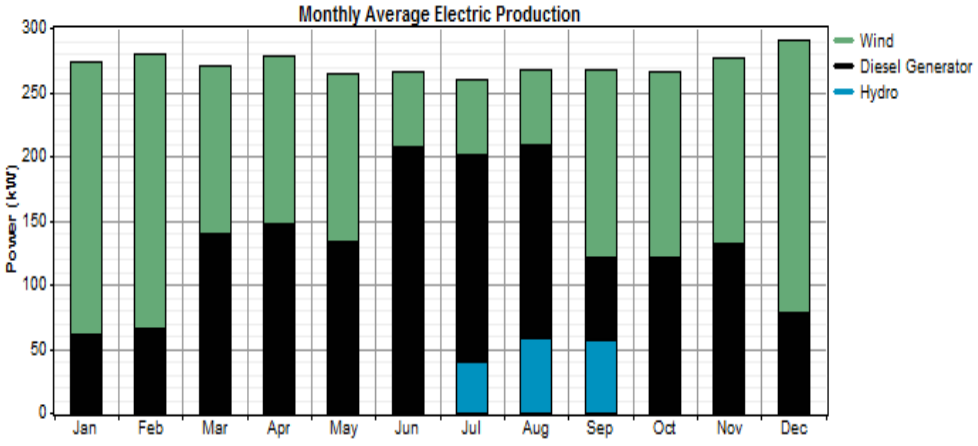

Figure 2-16: Power production in Case-3 Microgrid

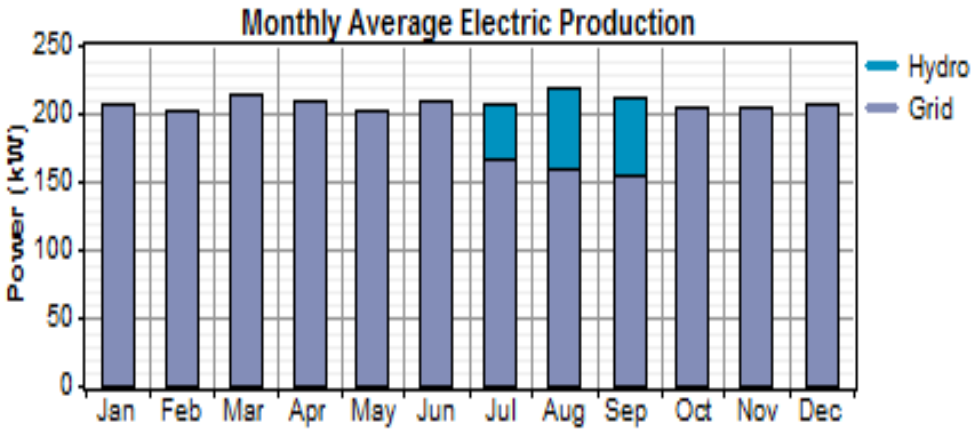

Figure 2-17: Power production in Case-4 Microgrid

2.6.1.3 Comparison of Environmental Emissions from Various Microgrid Configurations

As mentioned before, one of the main objectives of this work is to reduce emissions by using green energy sources. The results presented in Table 2-7 shown that the renewable microgrid in Case-2 significantly reduces the total system emissions as compared to all others cases. However, although Case-3 emits more than the renewable microgrid, it is still quite environmentally friendly when compared to the diesel microgrid.

Table 2-7: Case-wise comparison of emission

Emissions, ton/yr				
Pollutant	**Case-1**	**Case-2**	**Case-3**	**Case-4**
Carbon dioxide	6004.76	3.67	1078.4	1,086.18
Carbon monoxide	14.82	0	2.649	0
Unburned hydrocarbons	1.64	0	0.293	0
Particulate matter	1.12	0	0.2	0
Sulfur dioxide	12.06	0.008	2.17	4.7
Nitrogen oxides	132.23	0	23.64	2.29

2.6.2 Sensitivity Analysis

2.6.2.1 Effect of Unmet Energy

The effect of a capacity shortage on the microgrid is examined by allowing a small fraction of the annual load to remain unmet and determining the corresponding optimal microgrid plan, for Case-3. Two scenarios are formulated, one in which the maximum allowable unmet energy in the microgrid is 5% of the load, and the second, which has a maximum allowable unmet energy of 10%. Simulations are carried out using HOMER to determine if the optimal microgrid plan of Case-3, which comprises a mix of renewable energy and diesel, is affected by the allowable margins of unmet energy. The optimal microgrid plans presented in Table 2-8 shows that there is a substantial change when the allowable margin of unmet energy is 5%. The diesel and wind generation capacity is significantly reduced in the later case. However, when the allowable unmet energy limit is relaxed to 10%, there is no further change in microgrid plan.

The variation in NPC and other cost components are presented in Table 2-9. It is observed that the NPC and the levelized cost of energy reduces somewhat, when allowable unmet energy is 5% but does not change for the 10% unmet scenario. However, the operation cost increases slightly in the presence of unmet energy because of increased utilization of diesel generation, as seen in Table 2-10. It is also to be noted that the actual unmet energy in the system is much lower than the allowable limit of 5% and 10% respectively, in the two cases. The microgrid indeed seeks to meet the demand optimally from its available resources as far as possible even when the unmet energy margin is relaxed.

Table 2-8: Comparison of Case-3 optimal plan variation with unmet energy

Component	Case-3 (No unmet energy)	Maximum allowable unmet energy = 5%,10%
Diesel, kW	4,250	2,125
Solar PV, kW	0	0
Wind, kW	1000	500
Converter, kW	500	100
Battery, numbers	10,000	1,000

Micro-Hydro, kW	92	92
External Grid, kW	0	0

Table 2-9: Comparison of Case-3 cost components variation with unmet energy

Items	Case-3 (No unmet energy)	Maximum allowable unmet energy = 5%, 10%
Net Present Cost, M$	6.486	5.476
Levelized cost of energy,$/kWh	0.278	0.239
Operating Cost, M$/year	0.347	0.384

Table 2-10: Comparison of Case-3 production and consumption variation with unmet energy

	Production, MWh/yr	
Component	**Case-3 (No unmet energy)**	**Maximum allowable unmet energy = 5%, 10%**
Diesel Generator	1,107.04 (46%)	1,410,693 (66%)
Solar PV	0	
Wind	1,192.48 (49%)	596,238 (28%)
Micro-Hydro	115 (5%)	115 (5%)
External Grid	0	0
Renewable Energy Contribution	53.8%	33%
Total	2,414.51	2,122
	Consumption, MWh/yr	
Electrical Load Energy Served	1,825	1,792
Thermal Load Energy Served	182.5	182.5
Excess Energy to dump load	407.01	147.5
Unmet Energy	0	32.731

2.6.2.2 Effect of Diesel Price

Figure 2-18 shows that increase in diesel price has a significant effect on the NPC. From a base price of 0.3 $/L when the NPC is 6.48 million dollars, the NPC increases almost linearly as a function of the diesel price. At a price of 0.6 $/L, the NPC is 7.8 million dollars, which is a 20% increase in NPC for a 100% increase in diesel price. However, it may be noted that increase in diesel price can significantly reduce the emissions by altering the selection of energy supply options and shifting away from diesel to renewable energy generation. Increasing the diesel price to significantly high levels may also result in a reduction in NPC because of complete new selection of microgrid supply options.

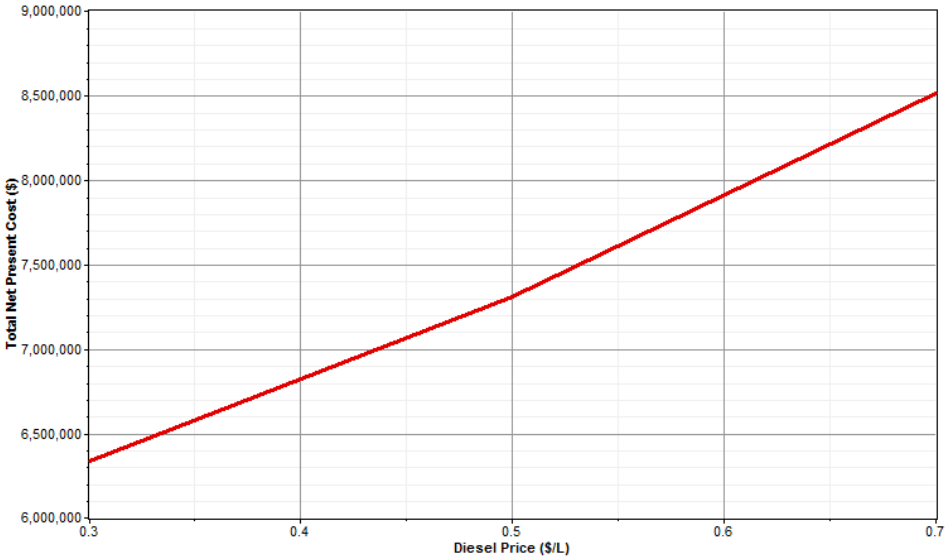

Figure 2-18: Total Net Present Cost vs. Diesel Price

2.6.2.3 Effect of Distance from Grid and the Optimal Breakeven Distance

In this analysis, the distance of the proposed microgrid site is taking into consideration and the optimal plan of Case-3 is determined assuming that the microgrid can draw power from the external grid. Figure 2-19 shows that the NPC of Case-3 microgrid, with grid connectivity option, is significantly less when the microgrid is very close to the external grid point of connection (say, zero kilometers). As the grid connectivity distance increases, the

NPC increases, but remains lower than the one without external grid option for up to 153 kms. Beyond that, it is no longer economical for the Case-3 microgrid to connect to the external grid.

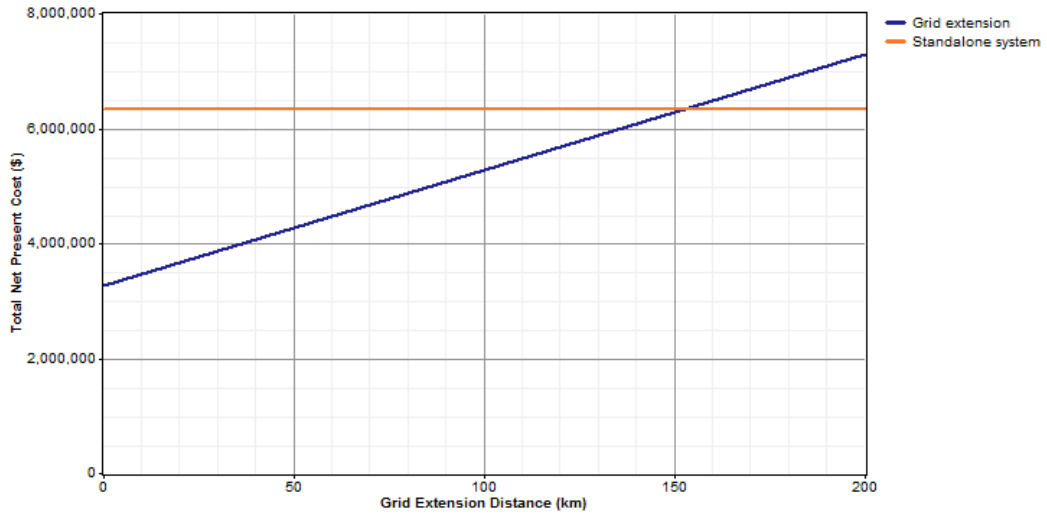

Figure 2-19: Variation of NPC with grid connectivity distance for Case-3 microgrid

2.7 Concluding Remarks

This chapter presents the optimal design and comparative studies for a diesel-only, a fully renewable-based, a diesel-renewable mixed, and an external-grid connected microgrid configuration. Various renewable energy options such as solar photo-voltaic (PV), wind, micro-hydro and batteries are considered as possible options in the microgrid supply plan. Studies are carried out using the HOMER software which provides a very efficient tool for case studies and policy analysis.

Analysis reveal that the diesel-renewable mixed microgrid has the lowest net present cost (NPC) and a fairly small carbon footprint, when compared to a stand-alone diesel-based microgrid. Although a fully renewable-based microgrid, which has no carbon footprint, is the most preferred, the net present cost (NPC) is higher.

Analysis is also carried out to determine the break-even grid extension distance from the microgrid location. It is observed that when the microgrid is connected to the external grid (Case-4), it is the most economically favorable option because of the fact that there is no

capital cost involved, and its operation and maintenance costs are much less compared to the diesel-based microgrid. In addition, the most environmentally friendly microgrid is the renewable energy microgrid (Case-2), and it results in significant savings in system emissions.

It is to be noted that there is still much work to be done in terms of renewable energy and mixed system development, because of their high initial capital and replacement costs. For example, the governmental feed-in tariffs will play a significant role in the renewable energy system cost. This work also demonstrates that allowing a small amount of annual load to be left unmet makes the microgrid (Case-3) more cost-effective. Also, the break-even distance presented in this chapter shows that for isolated microgrids, far away from the external grid connectivity point, the mixed microgrid (Case-3), is the most economic optimal choice. Finally, HOMER is found to be a very helpful tool for the microgrid planning and dispatching.

Chapter 3
Optimal PHEV Charging and its Impact on Distribution Operation

3.1 Introduction

Reducing global warming and GHG emissions is one of the major drives for the development of PHEVs. The price of oil reaching its highest levels, and the desire to reduce CO_2 emissions, are among the leading reasons for the increasing penetration of PHEVs. Increased numbers of PHEVs can have a significant impact on the distribution system performance such as reduction in power quality and efficiency, increase in power losses and voltage variations, as well as an adverse impact on the customers' energy price.

Therefore, meeting the increased demand arising from charging of the PHEVs while satisfying the distribution system operating constraints and reducing the system losses is a major challenge for distribution operators. Moreover, as utilities establish the TOU prices and Smart Grid communications networks, it allows them to move from a classical monthly billing cycle to dynamic pricing and TOU billing models. From PHEV customers point of view, minimization of the cost associated with PHEV charging, is the main objective.

In this chapter, optimal charging strategies are developed from two different perspectives. First, from the perspective of the distribution utility, where the objective is to minimize losses and second, from the perspective of the PHEV customer with the objective of minimizing cost.

This chapter is organized as follows. In Section 3.2, the mathematical model for determining the optimal PHEV charging, considering a typical distribution system is presented. In Section 3.3 the distribution system topology is presented and the analysis and case study is discussed in Section 3.4. The results and discussions are presented in Section 3.5. Finally, concluding remarks are presented in Section 3.6.

3.2 Mathematical Model for System Operation including PHEV

To solve the nonlinear relationships between the bus voltages and angles, power flow on the feeders, and the system demand, a power flow analysis is performed to determine the voltage deviations and power losses as well as the customers' energy cost.

3.2.1 Objective function

Two different objective functions are considered for analysis. The minimization of feeder losses, given by Equation (3.1) is the desired objective from the perspective of the distribution company.

$$Losses = \frac{1}{2} \sum_{k=1}^{24} \left\{ \sum_{i=1}^{N} \sum_{j=1}^{N} G_{i,j} \times [V_{i,k}^2 + V_{j,k}^2 - 2\ V_{i,k}\, V_{j,k} \cos(\delta_{j,k} - \delta_{i,k})] \right\} \qquad (\mathbf{3.1})$$

In (3.1), *k* is the index for time, N denotes the total number of busses in the system, $G_{i,j}$ is the conductance of feeder *i-j*.

The minimization of PHEV charging cost, given by Equation (3.2) is representative of the customers' desired objective.

$$\text{Cost} = \sum\nolimits_{\text{i}} \sum_{\text{k}}^{\text{Ek}} \text{Pch}_{\text{i,k}} * \text{Price}_{\text{k}} \qquad (\mathbf{3.2})$$

In (3.2), E_k is the end hour of the charging period, $Pch_{i,k}$ is the active power demand arising from the charging of the PHEVs batteries. And $Price_k$ is the TOU price [58].

3.2.2 Demand Supply Balance

Demand supply balance for both active and reactive power is given by the standard load flow equations as follows.

$$PG_{i,k} - PD_{i,k} = \sum_{j=1}^{N} V_{i,k}\, V_{j,k}\, Y_{i,j}\ \cos(\theta_{i,j} + \delta_{j,k} - \delta_{i,k}) \qquad (\mathbf{3.3})$$

$$QG_{i,k} - QD_{i,k} = -\sum_{j=1}^{N} V_{i,k}\, V_{j,k}\, Y_{i,j}\ \mathrm{Sin}(\theta_{i,j} + \delta_{j,k} - \delta_{i,k}) \qquad (\mathbf{3.4})$$

In equations (3.3) and (3.4), $PG_{i,k}$ and $QG_{i,k}$ are the active and reactive power injected by the generation buses at hour *k*, $PD_{i,k,}$ $QD_{i,k}$ are the active and reactive power demand at a bus at hour *k*. $Y_{i,j}$ is the admittance matrix element and $\theta_{i,j}$ is the corresponding angle.

3.2.3 Bus Voltage Limits

The voltage magnitudes at each bus at hour *k*, are constrained by their respective upper and lower limits, as follows.

$$\mathbf{V_i^{Min}} \leq \mathbf{V_{i,k}} \leq \mathbf{V_i^{Max}} \qquad (\mathbf{3.5})$$

These voltage ranges are applied to all load busses. On the other hand, the slack bus voltage magnitude and voltage angle, which is the substation bus, are fixed as follows.

$$V_{s,k} = 1\ \mathrm{p.u.}, \qquad \delta_{s,k} = 0, \qquad s = \mathrm{Slack\ bus}$$

3.2.4 Substation Capacity Limits

The substation capacity limit determines the maximum and minimum power withdrawal capacity over the substation transformer.

$$\mathbf{PS_i^{Min}} \leq \mathbf{PS_{i,k}} \leq \mathbf{PS_i^{Max}} \qquad (\mathbf{3.6})$$

$$\mathbf{QS_i^{Min}} \leq \mathbf{QS_{i,k}} \leq \mathbf{QS_i^{Max}} \qquad (\mathbf{3.7})$$

In (3.6) and (3.7), $PS_{i,k}$ and $QS_{i,k}$ are the active and reactive power injected to the system through the substation transformers at hour *k*.

3.2.5 PHEV Operational Constraints

The demand supply balance constraint for each bus at hour *k*, is updated by adding the PHEV charging load to the active power demand supply balance as given by equation (3.8).

$$\mathbf{PG_{i,k} - PD_{i,k} - Pch_{i,k} = \sum_{j=1}^{N} V_{i,k}\, V_{j,k}\, Y_{i,j}\ \cos(\theta_{i,j} + \delta_{j,k} - \delta_{i,k})} \qquad (\mathbf{3.8})$$

$Pch_{i,k,}$ the active power load introduced by the charging of the PHEVs batteries, is a variable, determined from the model solution.

The PHEV charger output power constraint is given as follows:

$$\mathbf{Pch_i^{Min} \leq Pch_{i,k} \leq Pch_i^{Max}} \qquad (\mathbf{3.9})$$

The total charging output power during a period is limited by the PHEV battery capacity, as given by Equation (3.10).

$$\mathbf{\sum_{k}^{Ek} Pch_{i,k} = C_{battery}^{Max}} \qquad (\mathbf{3.10})$$

In Equation (3.10), $C_{Battery}^{Max}$ is the PHEV battery capacity.

This model can also consider feeder thermal limits, but in such cases where there is a need to have more decision variables- such as PHEV options, this limit is relaxed in order to arrive at a feasible solution set.

The above NLP model is solved using the MINOS5.1 solver in the GAMS environment.

3.3 Distribution System Topology

The analysis reported in this chapter is carried out considering a radial distribution system, the 69-bus system [59], whose single line diagram is shown in Figure 3-1. The distribution system is supplied through the substation at bus-1. The detailed data containing the active

and reactive power components of the load at each receiving end bus as well as the resistance and reactance parameters of the feeders are provided in reference [59].

It is assumed that a PHEV charging station is located at bus-59, which can accommodate simultaneous charging of 1000 standard PHEV models. Each PHEV impose a maximum electrical load of 4 kW on the system, which implies a maximum total additional load of 4 MW at bus-59.

Each PHEV has a charging energy of 9.65 kWh which means, the total charging energy required by the PHEV charging station in any given period, for 1000 vehicles, is 9.65 MWh. The above typical values are considered for level-2 charging which is 240 V distribution system [21]. The model presented in Section-3.2 and the analysis reported hereafter, are generic enough, and similar conclusions may be drawn for a 110 V distribution system as well.

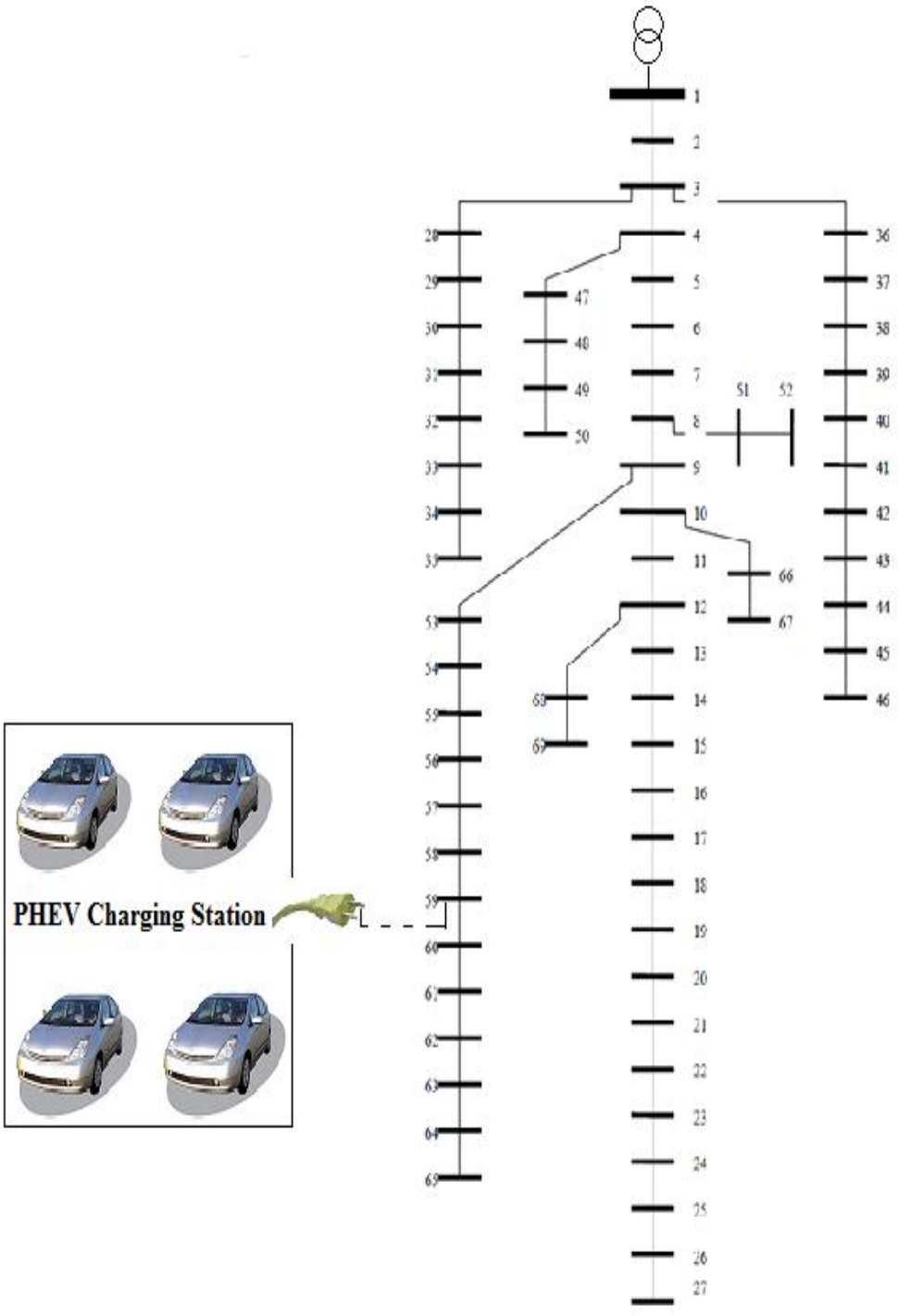

Figure 3-1: 69-Bus radial distribution system [59]

3.3.1 Load profile

A 24-hour load profile is assumed for the distribution system. A simplifying assumption is made that all bus loads have the same chronological load profile, as shown in Figure 3-2.

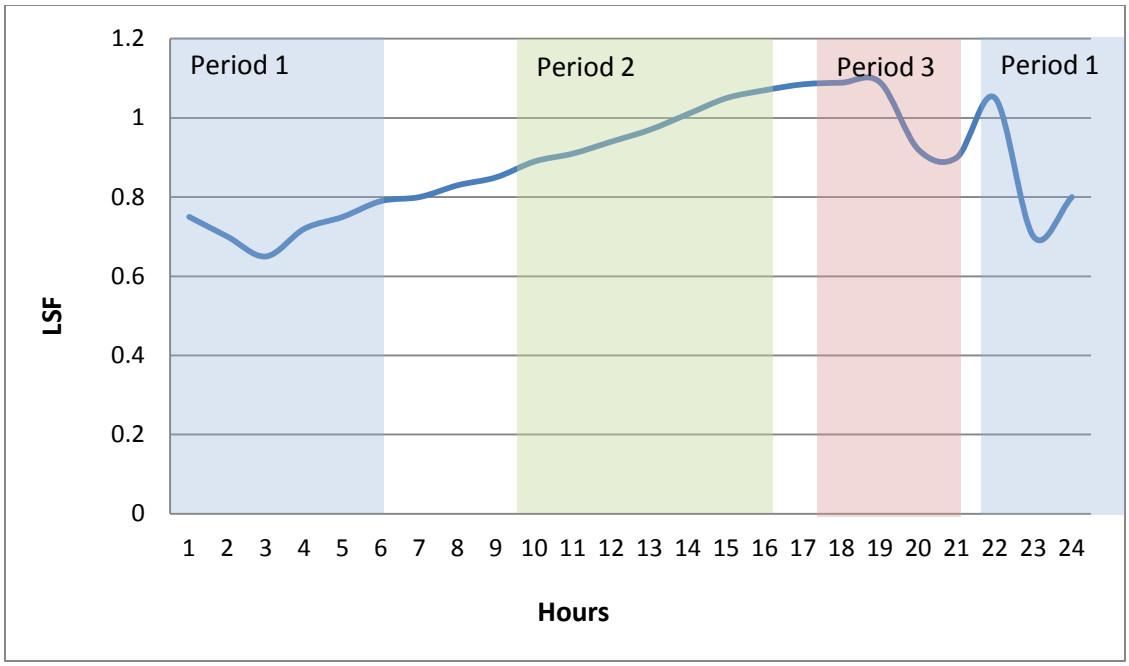

Figure 3-2: Load scale factors for the distribution system bus loads

3.3.2 Time-of-Use Pricing

The Ontario TOU price structure for both summer and winter rates are used in this work, as shown in Figure 3-3 [58]. It is observed that the TOU price structure represents the typical energy use profile of Ontario customers, and is also governed by the climatic conditions. In summer, the peak price appears during the afternoon (11 AM – 5 PM) primarily because of air-conditioning loads, while in the winter the peak price appears in the morning (7 AM – 11 AM) and evening (5 PM – 10 PM) because of heating loads.

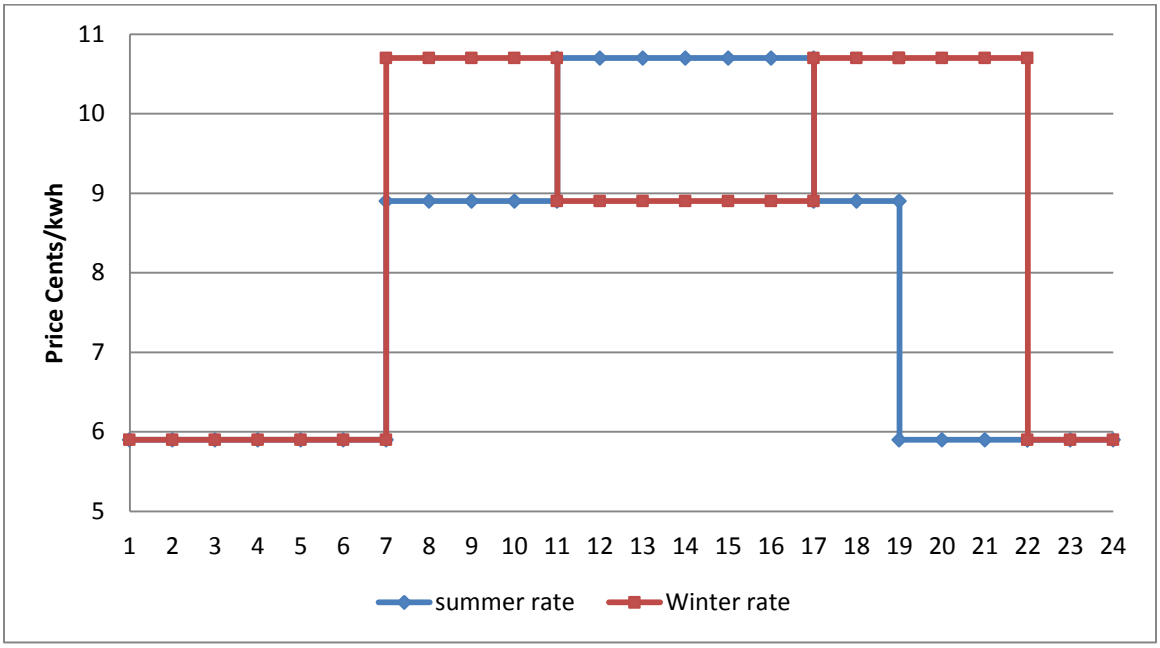

Figure 3-3: Time-of-Use prices for winter and summer in Ontario [58]

3.4 Definition of Scenarios

In this chapter three scenarios are constructed, and three different charging periods are considered, to examine the impact of charging PHEVs under different system load conditions, as given below:

- Period-1: Midnight – 6 AM, 10 PM – midnight.
- Period-2: 10 AM – 4 PM.
- Period-3: 6 PM – 9 PM.

The PHEVs batteries are assumed to be fully discharged at the start of each period and are fully charged at the end of the period. The start and end time of the charging process is not fixed, but is required to be completed within a period. Therefore, the optimal charging amount and duration in each period, is determined from the proposed model. This can be implemented by sending a signal from and to the smart meter to the PHEV [22].

3.4.1 Scenario 1: Base Case

In this scenario, no PHEVs are assumed, and hence this is considered as the Base case. Therefore, the OPF model developed in Section-3.2 is applied to the 69-bus distribution system with minimizing losses as the objective function, without the PHEV operation constraints of Section-3.2.5.

3.4.2 Scenario 2: With PHEVs and Minimizing Losses

In this scenario the electrical load associated with charging PHEVs at bus-59, is assumed to add an extra 4 MW of load. There is a significant impact of uncoordinated charging of PHEVs on the distribution system, thereby increasing the total system losses, peak demand, and adversely affecting the system voltage profile [46, 47]. In this scenario, coordinated charging of PHEVs is proposed by minimizing the total system losses.

3.4.3 Scenario 3: With PHEVs and Minimizing Customer Cost

In this scenario, the proposed OPF model including PHEV constraints of Section-3.2.5, is used considering the cost objective function, equation (3.2). Also in this scenario, both the summer and winter TOU rates of Ontario are considered, and their effects are examined.

3.5 Results and Discussions

As discussed in the previous section, Scenarios 2 and 3 examine the cases with PHEV charging station connected to the grid at bus-59. In this section, the optimal charging profiles obtained in these scenarios are examined in detail. Note that for Scenario 3, both summer and winter TOU prices are examined separately (Figure 3-4).

The charging decisions are obtained for each charging period, considered independent of each other, although the charging profiles presented in Figure 3-4 depict a 24-hour horizon.

As can be seen in Figure 3-4, the charging profile of the PHEVs in Scenario 2, is spread over the entire charging periods almost equally, and there is no effect of TOU prices that can be noted. On the other hand, the PHEV charging profiles in Scenario 3 changes significantly from hour to hour depending on the TOU prices, and do not require the entire charging period to charge the battery, and hence resulting in rapid charging.

It is also noted that there are significant differences in the charging profiles obtained using the summer TOU rates and the winter rates, for period-2 and 3, when there are seasonal differences in the rates.

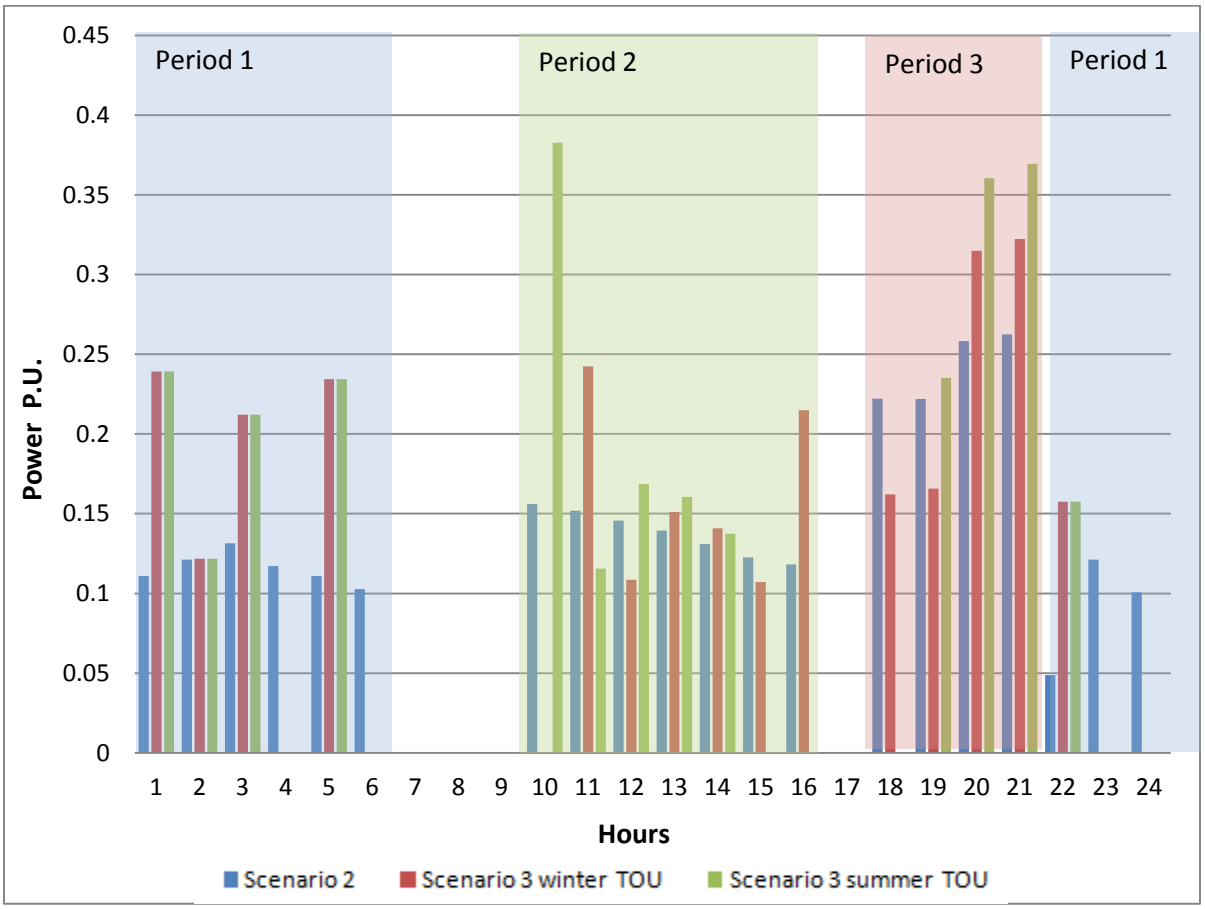

Figure 3-4: Optimal charging profile of PHEV in different scenarios

The total system losses for various cases are present in Table 3-1. As seen in Table 3-1, the Base Case has the lowest power losses because there is no PHEV charging, and hence no extra load arising in the system. When the PHEV load appears on the system in Scenario 2 and Scenario 3, comparing between various charging periods, it is noted that the system losses increase significantly, if PHEV charging is considered in period 3, which is the peak load period. If PHEVs are scheduled for charging during period 2, which is during the morning hours with medium load, system losses are lower in all the scenarios. The most favorable charging cycle is during period 1, the overnight off-peak load.

Comparing across the scenarios, it is noted that there is a significant saving in the total system losses in Scenario 2 as compared to Scenario 3 in all charging periods. In addition, the different seasonal TOU prices play a significant role in the total system losses; for example, charging the PHEVs during period 2 and 3 in winter, results in larger saving in total system losses in comparison to summer.

Table 3-1: Total system losses (MW)

Period	Scenario 1	Scenario 2	Scenario 3	
			Summer TOU	Winter TOU
1	3.847	4.538	5.453	5.453
2		4.945	6.160	5.703
3		5.400	6.454	6.061

The hourly plots of system losses for Scenarios 2 and 3 for PHEV charging to take place during period 3 are presented in Figure 3-5. It is seen that, because of the charging load, the losses is increase during the period, for both the scenarios. However significantly higher losses are noted in Scenario 3 with summer TOU prices, because during period 3, hours 19 – 21, the summer TOU prices are at their minimum, and more intense charging taken place during these hours, as also evident from Figure 3-5.

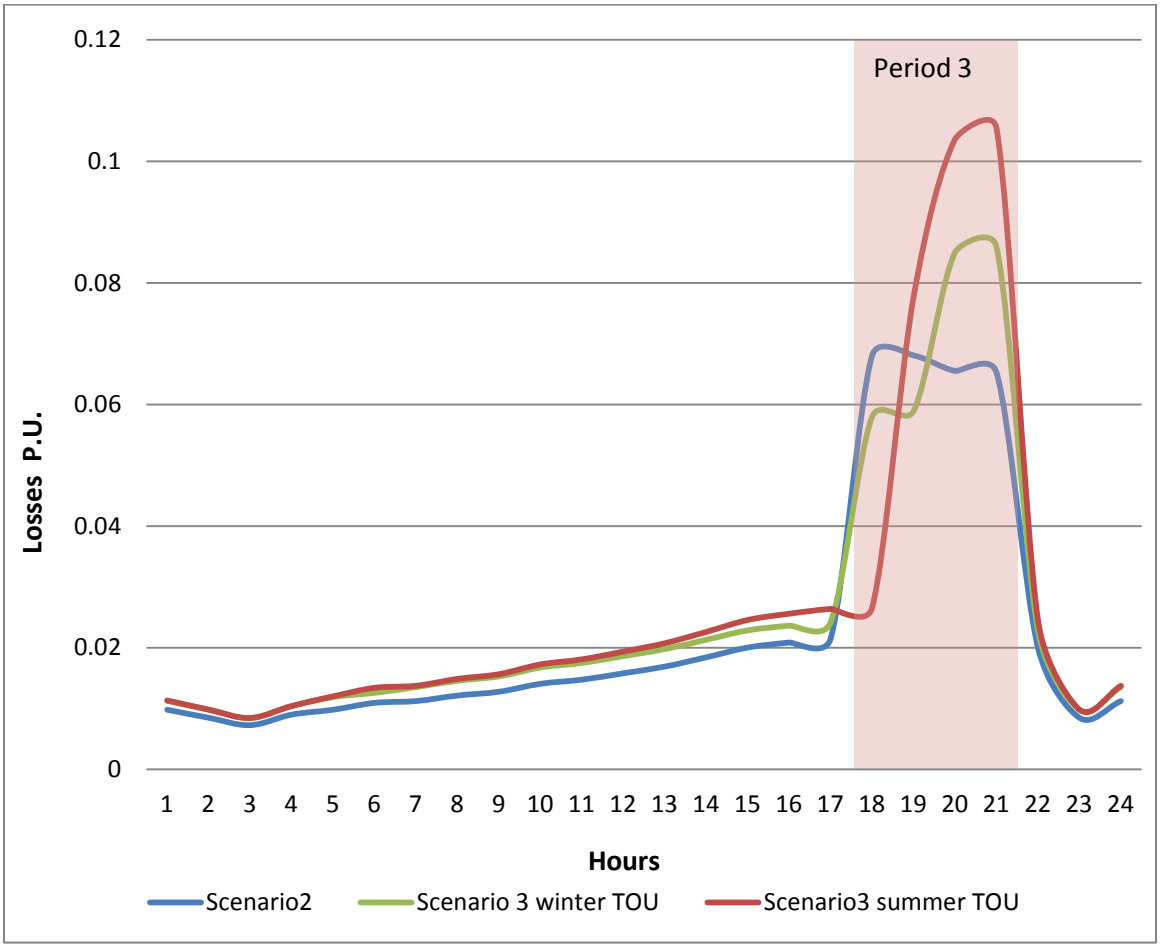

Figure 3-5: System Losses for Scenarios 2 and 3 During Period 3

Table 3-2 presents a comparative summary of the total PHEV charging costs incurred in the two scenarios, for each charging period. As expected, Scenario 3 which minimizes the PHEV charging cost, results in minimum costs for periods 2 and 3 for both summer and winter TOU prices. However, there is no change in the PHEV charging cost during period 1 in between the two scenarios.

Table 3-2: Total PHEV charging cost, $

Period	Scenario 2		Scenario 3	
	Summer TOU	Winter TOU	Summer TOU	Winter TOU
1	569.35	569.35	569.35	569.35
2	1004.439	886.961	963.65	858.85
3	636.003	1032.55	569.35	1032.55

The Figures 3-6 to 3-8, present the voltage profiles at some specific buses for the charging periods to examine the impact of PHEV charging in various Scenarios.

It is seen that PHEV charging in Scenario 3 during period 3 results in some voltage drop, but the voltage drop is significant if PHEV charging is in period 2. For example, bus-65 which is a remote bus and located near the PHEV charging station, is the one most affected with its voltage at close to the lower allowable limit of 0.90 p.u. during period 2 and period 3.

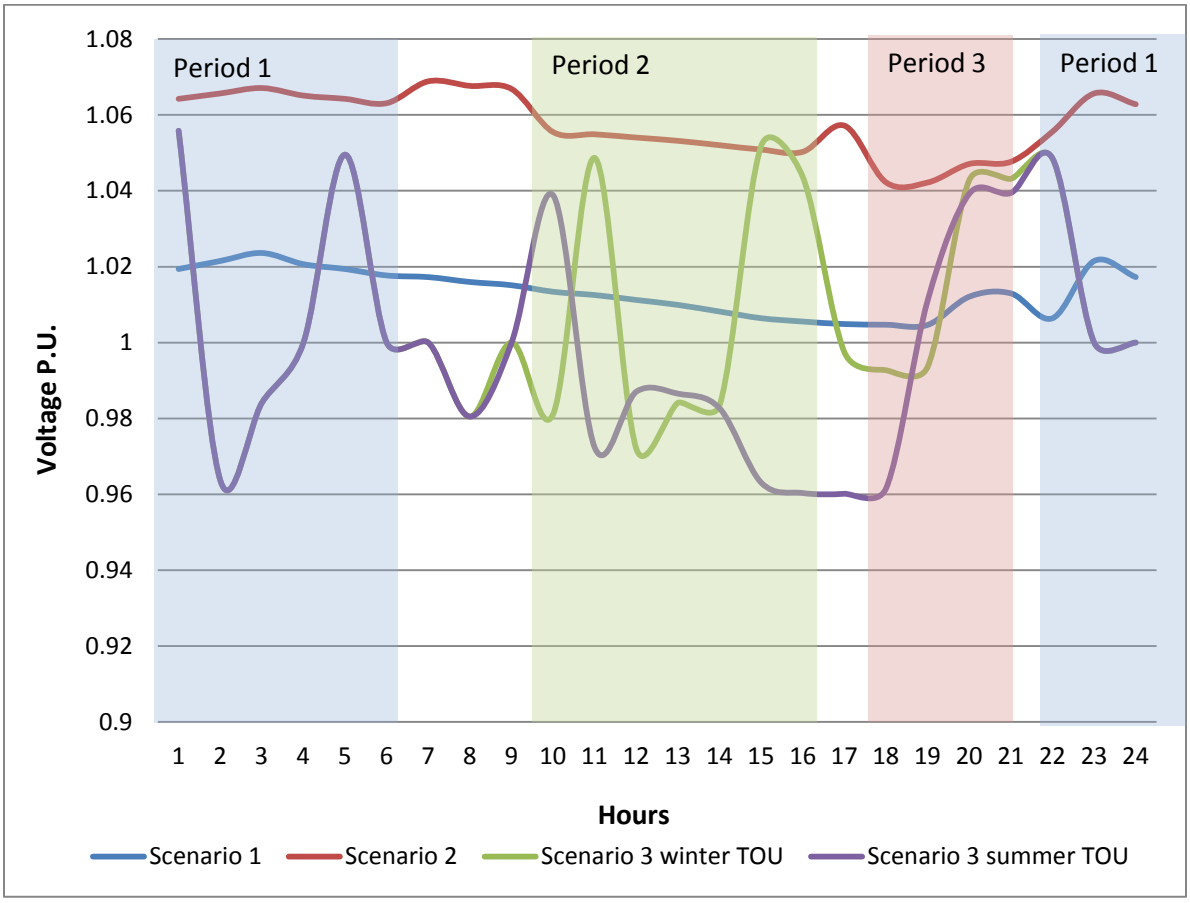

Figure 3-6: Voltage profile at bus 27

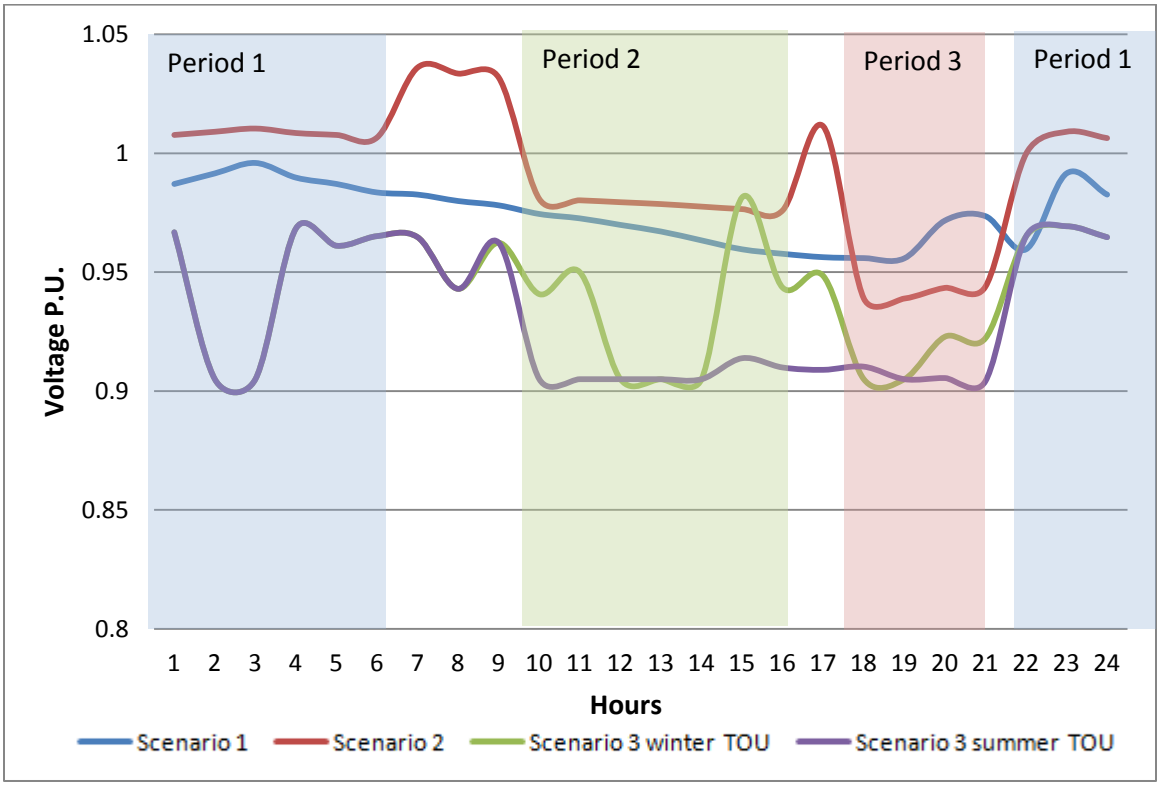

Figure 3-7: Voltage profile at bus 65

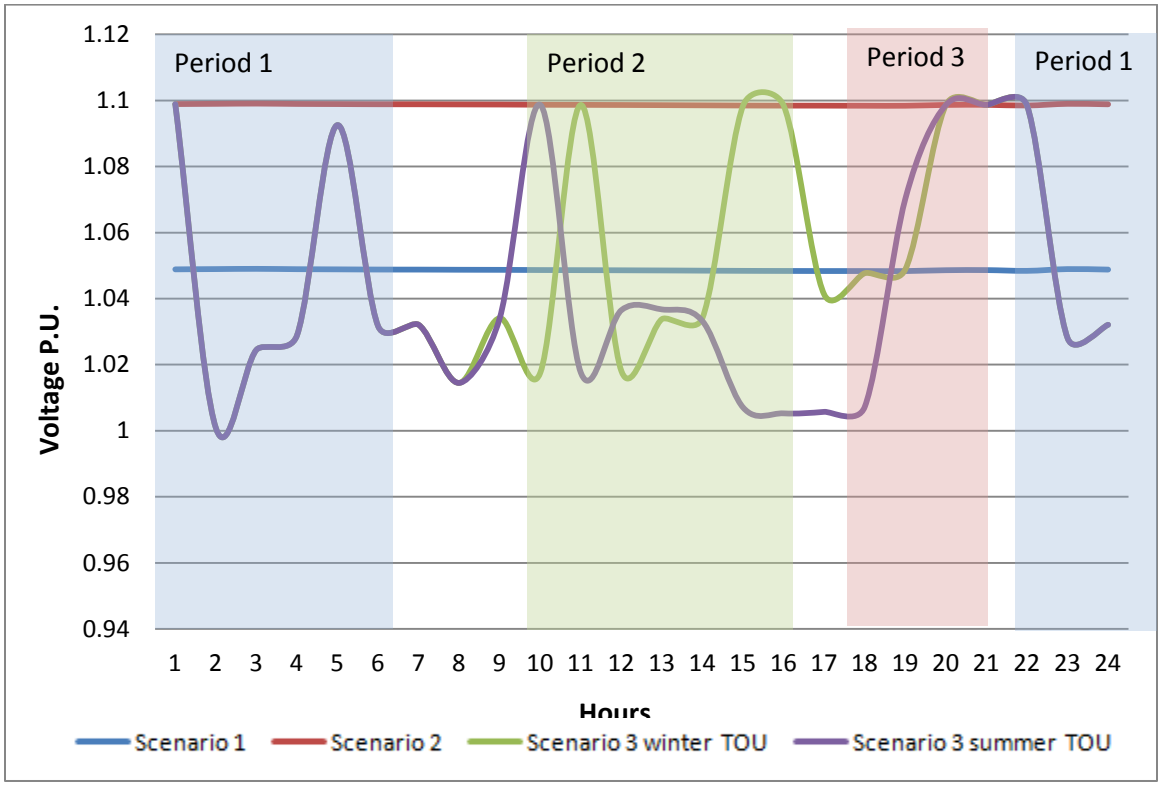

Figure 3-8: Voltage profile at bus 46

Figure 3-9 presents the active power transferred through the transformer for various scenarios. As expected, when the PHEV charging is taking place in Scenario 2 the active power transferred through the transformer is increased for all periods as compared to the Base Case. However, increase in the active power transfer through the transformer is significant if PHEV charging is considered in Scenario 3. It is noted that in Scenario 3 and summer TOU rate, the transformer operates close to its upper allowable limit.

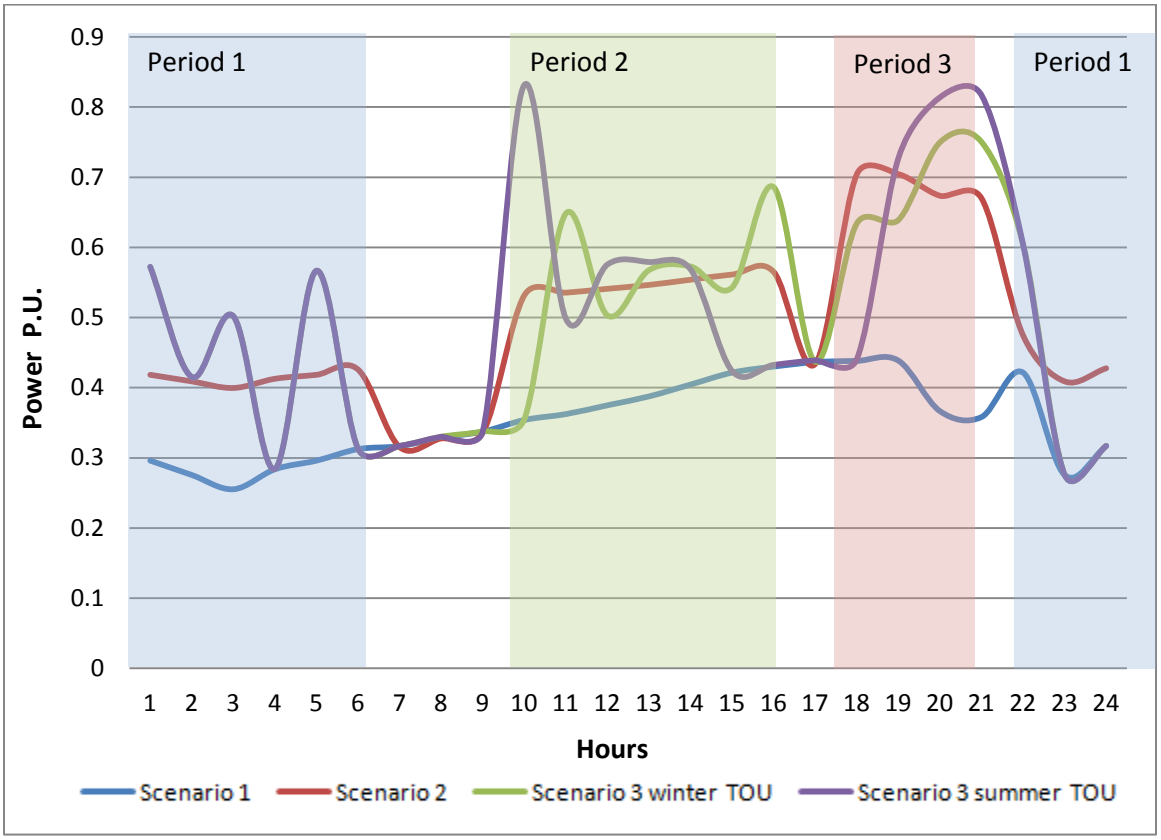

Figure 3-9: Active power transfer over substation transformer

The reactive power transferred through the transformer for various scenarios are presented in Figure 3-10. It can observe that in Scenario 2, the reactive power transferred through the transformer is increased in comparison with the Base Case. The reactive power transferred through the transformer is increased even more in Scenario 3.

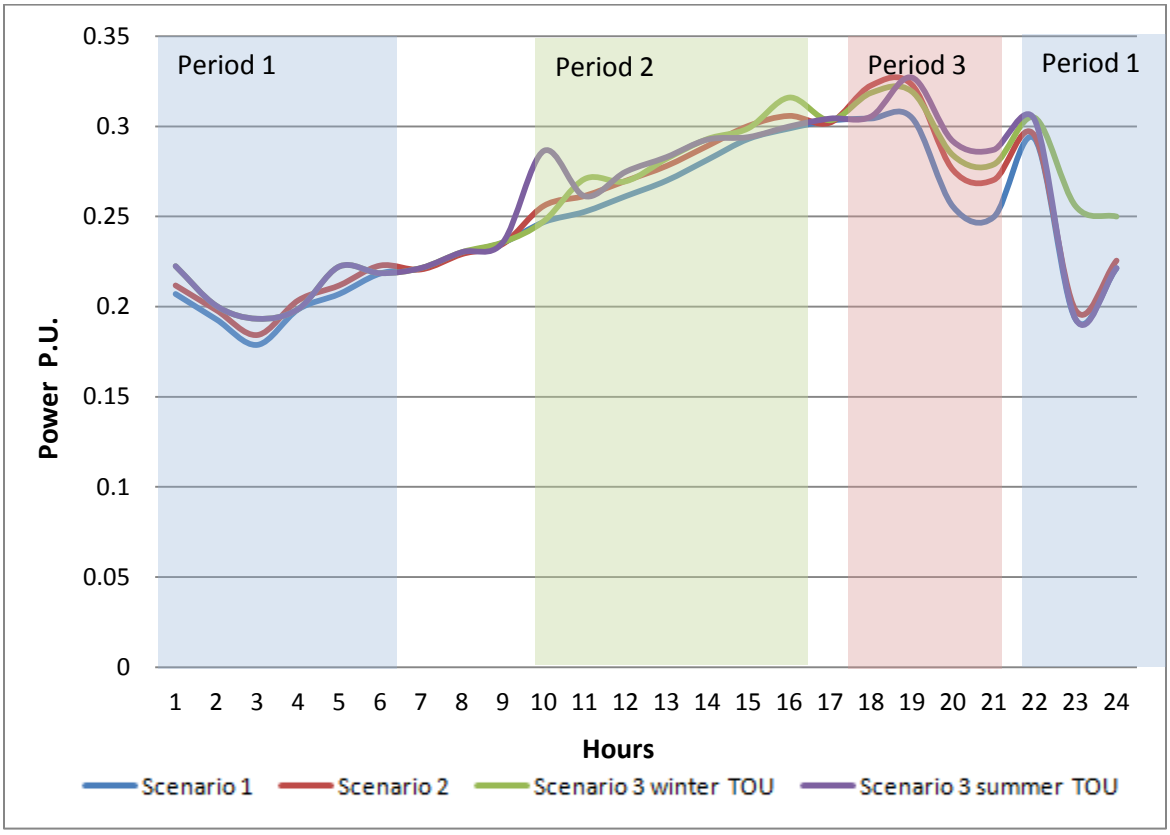

Figure 3-10: Reactive power transfer over substation transformer

3.6 Concluding Remarks

An optimal power flow model considering two different objectives, minimizing feeder losses and charging cost, while meeting distribution system constraints is presented in this chapter to understand the impact of PHEVs charging on distribution networks. A 24-hours day cycle distribution demand is attached with three different scenarios. Three different charging periods are investigated. The impacts of this extra load arising from charging PHEV to the distribution system such as, peak load, off-peak load, transformer active and reactive power output, bus voltage drop, and the PHEV customer cost are investigated.

From the results conducted in this chapter it can observed that, charging the PHEVs during period 1, is not significantly affected the daily operation of the proposed distribution system and it is the most favorable charging period because it has the minimum total system

losses, as well as minimum cost in comparison to the others charging periods. If PHEV charging is considered during period 2, which is happening during morning time, does not create significant problems in terms of reliable operation of this proposed distribution system. However, if PHEV is scheduled for charging during period 3, which is charging during peak time, could have an unfavourable impact such as maximum total system losses, although large voltage deviation and a high charging cost compared with periods 1 and 2.

The purpose of this study was to investigate an optimal operation strategy for a distribution system using GAMS simulation. This work demonstrated that charging during overnight period 1 will make the mentioned distribution system more reliable and have reduction in the PHEV customer cost. Also, optimal charging profile is determined using the proposed model. Finally, the proposed optimal load flow model is found to be a very helpful tool for examined the mentioned distribution system coupled with PHEVs charging impact.

Chapter 4

Optimal PHEV Charging in Coordination with Distributed Generation Operation in Distribution Systems

4.1 Introduction

In Chapter 3, the impact of penetration of PHEV on the distribution system is discussed in details from the perspective of the distribution utility, where the objective is to minimize losses and from the perspective of the PHEV customer with the objective of minimizing charging cost. It is found that the presence of charging PHEVs, can significantly affect the distribution system performance as well as customer cost. As the DG resources are becoming an important alternative to the power developers, the impact of renewable energy sources combined with PHEV have to be carefully examined. Renewable energy sources such as solar and wind can help the distribution system performance, for example, it can improve the system quality by reducing the system losses, voltage deviation, transformers and feeders overloading. While, these energy sources can help meet the requirements of PHEV charging and significantly maximize the PHEV customer savings, because of their intermittent and non-dispatchable nature, the charging periods need to be carefully determined.

In this chapter, the contribution of the renewable energy sources is computed in terms of the incremental reduction in system loss for any incremental injection of active power from these green energy sources. Furthermore, in order to figure out the optimal charging periods of PHEVs as well as the impact of renewable energy sources, the model developed in the previous chapter, has been used in this chapter as well but, the system constraints are modified considering the contribution of renewable energy sources.

The rest of this chapter is organized as follows. The system model and constraints is presented in Section 4.2. In Section 4.3, the system information as well as the renewable energy sources data is presented. The results and discussions are presented in Section 4.4. Finally, concluding remarks are presented in Section 4.5.

4.2 System Model

4.2.1 Wind Model

The ideal power curve for wind turbines is given by Figure 4-1 [16].

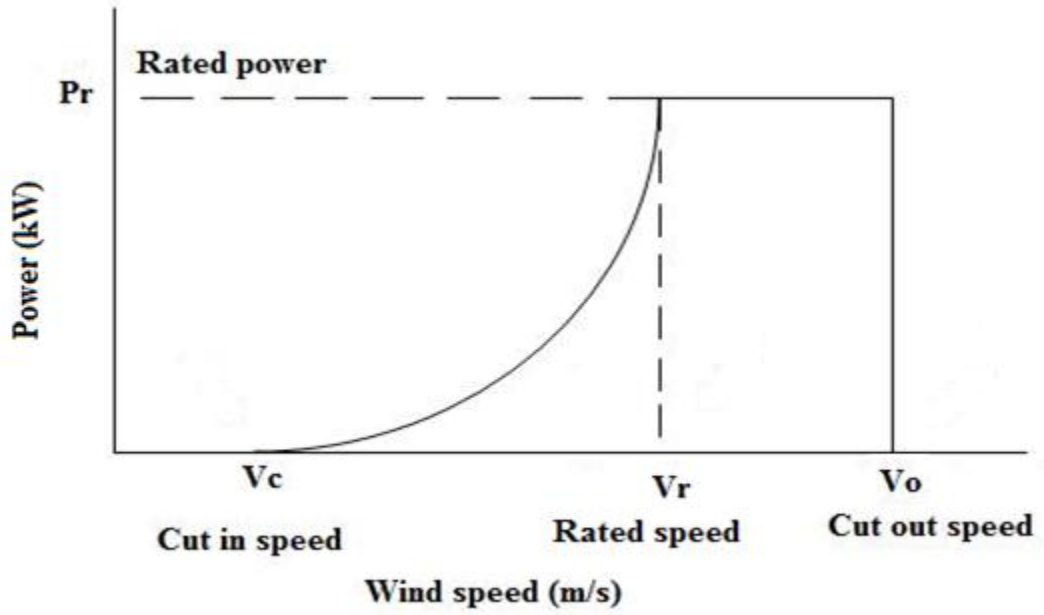

Figure 4-1: Wind turbine ideal power curve [16]

In this work it is assumed that the cut-in wind speed is 4 m/s, the rated wind speed is 16 m/s and cut-out wind speed is 25 m/s. Moreover, after the wind speed at the site is determined and the different parameters of the wind turbine ideal power curve are known, then the generation of active power from wind turbine can be expressed numerically using equation (4.1).

$$P_w = \begin{cases} 0 & 0 \le v \le v_c \\ L(v) & v_c \le v \le v_r \\ P_{rated} & v_r \le v \le v_o \\ 0 & v \ge v_o \end{cases} \quad (4.1)$$

Where the function L(v) can be calculated using equation **(4.2)**.

$$L(v) = (a + b\,v + c\,v^2)P_{rated} \quad (4.2)$$

In the above equation P_{rated} is the rated power output of the wind turbine and is assumed 1000 kW and the a, b and c parameters are constant terms and can be expressed in terms of v_c and v_r as given by equations (4.3-4.5) [60].

$$\mathbf{a} = \frac{1}{(\mathbf{v_c} - \mathbf{v_r})^2}\left[\mathbf{v_c}(\mathbf{v_c} + \mathbf{v_r}) - \mathbf{4}\,\mathbf{v_c}\,\mathbf{v_r}\left(\frac{\mathbf{v_c} + \mathbf{v_r}}{\mathbf{2v_r}}\right)^{\mathbf{3}}\right] \quad \textbf{(4.3)}$$

$$\mathbf{b} = \frac{1}{(\mathbf{v_c} - \mathbf{v_r})^2}\left[\mathbf{4}(\mathbf{v_c} + \mathbf{v_r})\left(\frac{\mathbf{v_c} + \mathbf{v_r}}{\mathbf{2v_r}}\right)^{\mathbf{3}} - (\mathbf{3v_c} + \mathbf{v_r})\right] \quad \textbf{(4.4)}$$

$$\mathbf{c} = \frac{1}{(\mathbf{v_c} - \mathbf{v_r})^2}\left[\mathbf{2} - \mathbf{4}\left(\frac{\mathbf{v_c} + \mathbf{v_r}}{\mathbf{2v_r}}\right)^{\mathbf{3}}\right] \quad \textbf{(4.5)}$$

4.2.2 Solar Model

This section presents the calculation of the output of active power from the PV module. The output power of the PV module can be calculated as given by equation (4.6).

$$\mathbf{P_s} = \mathbf{P_{rated}}\,\mathbf{D_f}\left(\frac{\mathbf{R_t}}{\mathbf{R_{standard}}}\right)\left[\mathbf{1} + \boldsymbol{\alpha}_\mathbf{p}(\mathbf{T_{pv}} - \mathbf{T_{standard}}\right] \quad \textbf{(4.6)}$$

Where P_s is the output power from the PV module, P_{rated} is the rated power output of the PV module and is assumed 500 kW, D_f is the derating factor of the PV and it is assumed to be equal 90%, which reduces the PV production by 10% to approximate the varying effects of temperature and dust on the panels. R_t and $R_{standard}$ are respectively, the solar radiations during hour *t* and the radiation under standard test condition which is 1 kW/m^2. Also, α_p is the temperature coefficient of power and T_{pv} and $T_{standard}$ are respectively, the panel temperature and the panel temperature under standard test condition which is 25°C. For simplicity, the temperature coefficient of power is assumed to be zero in this work, so that simplifies the equation **(**4.6**)** to the following equation [30].

$$\mathbf{P_s} = \mathbf{P_{rated}}\,\mathbf{D_f}\left(\frac{\mathbf{R_t}}{\mathbf{R_{standard}}}\right) \quad \textbf{(4.7)}$$

4.2.3 OPF Model for System Operation Including PHEV, Wind and solar

To solve the nonlinear relationships between the bus voltages and angles, power flow on the feeders, and the system demand, an OPF analysis is performed to determine the voltage deviations and power losses as well as the customers' energy cost.

Objective Function

Two different objective functions are considered for analysis. The minimization of feeder losses, given by Equation (4.8) is the desired objective from the perspective of the distribution company.

$$Losses = \frac{1}{2} \sum_{k=1}^{24} \left\{ \sum_{i=1}^{N} \sum_{j=1}^{N} G_{i,j} \times [V_{i,k}^2 + V_{j,k}^2 - 2\ V_{i,k}\, V_{j,k} \cos(\delta_{j,k} - \delta_{i,k})] \right\} \qquad (\mathbf{4.8})$$

In (4.8), *k* is the index for time, N denotes the total number of bus in the system, $G_{i,j}$ is the conductance of feeder *i-j*.

The minimization of PHEV charging cost, given by Equation (4.9) is representative of the customers' desired objective.

$$\text{Cost} = \sum_{i=1}^{N} \sum_{k}^{Ek} \text{Pch}_{i,k} * \text{price}_{k} \qquad (\mathbf{4.9})$$

In (4.9), E_k is the end hour of the charging period, $Pch_{i,k}$ is the active power demand arising from the charging of the PHEVs batteries, and $Price_k$ is the TOU price [58].

Demand Supply Balance

Demand supply balance for both active and reactive power is given by the standard load flow equations as follows.

$$PG_{i,k} - PD_{i,k} = \sum_{j=1}^{N} V_{i,k}\, V_{j,k}\, Y_{i,j}\ \cos(\theta_{i,j} + \delta_{j,k} - \delta_{i,k}) \qquad (\mathbf{4.10})$$

$$QG_{i,k} - QD_{i,k} = -\sum_{j=1}^{N} V_{i,k}\, V_{j,k}\, Y_{i,j}\ \mathrm{Sin}(\theta_{i,j} + \delta_{j,k} - \delta_{i,k}) \qquad (\mathbf{4.11})$$

In equations (4.10) and (4.11), $PG_{i,k}$ and $QG_{i,k}$ are the active and reactive power injected by the generation buses at hour *k*, $PD_{i,k,}$ $QD_{i,k}$ are the active and reactive power demand at a bus at hour *k*. $Y_{i,j}$ is the admittance matrix element and $\theta_{i,j}$ is the corresponding angle.

Bus Voltage Limits

The voltage magnitudes at each bus at hour *k*, are constrained by their respective upper and lower limits, as follows.

$$\mathbf{V_i^{Min}} \leq \mathbf{V_{i,k}} \leq \mathbf{V_i^{Max}} \qquad (\mathbf{4.12})$$

These voltage ranges are applied to all load busses. On the other hand, the slack bus voltage magnitude and voltage angle, which is the substation bus, are fixed as follows.

$$V_{s,k} = 1\ \mathrm{p.u.} \quad , \quad \delta_{s,k} = 0 \quad , \quad s = \mathrm{Slack\ bus}$$

Substation Capacity Limits

The substation capacity limit determines the maximum and minimum active and reactive power withdrawal capacity over the substation transformer.

$$\mathbf{PS_i^{Min}} \leq \mathbf{PS_{i,k}} \leq \mathbf{PS_i^{Max}} \qquad (\mathbf{4.13})$$

$$\mathbf{QS_i^{Min}} \leq \mathbf{QS_{i,k}} \leq \mathbf{QS_i^{Max}} \qquad (\mathbf{4.14})$$

In (4.13) and (4.14), $PS_{i,k}$ and $QS_{i,k}$ are the active and reactive power injected to the system through the substation transformers at hour *k*.

PHEV Operational Constraints

The demand supply balance constraint for the specific bus with the PHEV charging load at hour *k*, is updated by adding the PHEV charging load to the active power demand supply balance, as follows:

$$\mathbf{PG_{i,k} - PD_{i,k} - Pch_{i,k} = \sum_{j=1}^{N} V_{i,k}\, V_{j,k}\, Y_{i,j}\ \cos(\theta_{i,j} + \delta_{j,k} - \delta_{i,k})} \qquad (\mathbf{4.15})$$

$Pch_{i,k,}$ is the active power load introduced by the charging of the PHEV batteries, which is a variable, determined from the model solution.

The PHEV charger output power constraint is given as follows:

$$\mathbf{Pch_i^{Min} \leq Pch_{i,k} \leq Pch_i^{Max}} \qquad (\mathbf{4.16})$$

The total charging output power during a period is limited by the PHEV battery capacity, as given by Equation (4.17).

$$\mathbf{\sum_{k}^{Ek} Pch_{i,k} = C_{battery}^{Max}} \qquad (\mathbf{4.17})$$

In Equation (4.17), $C_{Battery}^{Max}$ is the PHEV battery capacity.

The model presented by equation (4.8)-(4.17) can also consider feeder thermal limits, but in such cases where there is a need to have more decision variables- such as PHEV options, this limit is relaxed in order to arrive at a feasible solution set.

Update the Model Constraints considering Renewable Energy Sources

The contribution of the renewable energy sources comprising wind turbines and solar PV arrays are included in the demand supply balance constraints, as below.

$$PG_{i,k} + P_{w,k} + P_{s,k} - PD_{i,k} - Pch_{i,k} = \sum_j V_{i,k}\, V_{j,k}\, Y_{i,j}\ \cos(\theta_{j,i} + \delta_{j,k} - \delta_{i,k}) \qquad \mathbf{(4.18)}$$

In equation (4.18), the $P_{w,k}$ and $P_{s,k}$ are the active power generated from the wind turbine and solar PV at hour *k*, respectively.

After the above constraints are updated the proposed model is re-run to calculate the optimal power flow in the system and the optimal charging amount and duration while minimizing the total system losses as well as the customers cost. The above NLP model is solved using the MINOS5.1 solver in the GAMS environment.

4.3 System Information

4.3.1 Distribution System Topology

The analysis reported in this chapter is carried out considering a radial distribution system, the 69-bus system [59], whose single line diagram is shown in Figure 4-2. The distribution system is supplied through the substation at bus-1.

It is also assumed that a PHEV charging station is located at bus-59 which can impose a maximum load of 4 MW, which is equivalent to charging 1000 standard PHEV models simultaneously, each of 4 kW load. The wind turbines are assumed to be connected at bus-65, while the solar panels are located at bus-50.

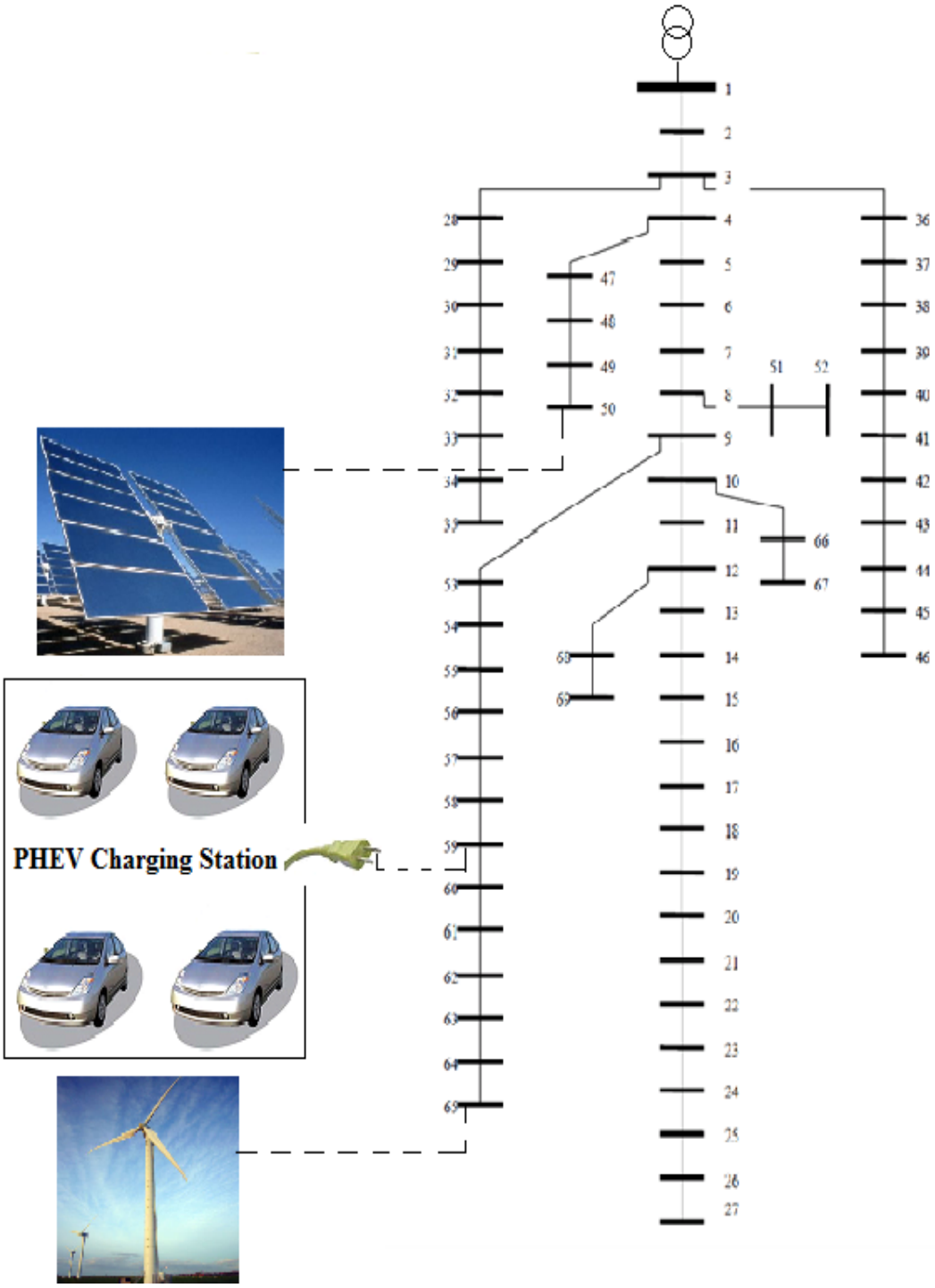

Figure 4-2: 69-Bus radial distribution system with renewable energy contribution [59]

4.3.2 Wind Source

The wind speed profile of Waterloo, Ontario, (43° 39' N, 80° 32' W) is obtained from the Canadian Wind Energy Atlas [57]. The annual average wind for this area is 5.78 m/s.

In this chapter two different daily profiles are used. The first profile considers high wind speeds, which occurs during the winter season. The second profile is selected from a typical summer day. The two different profiles are presented in Figure 4-3.

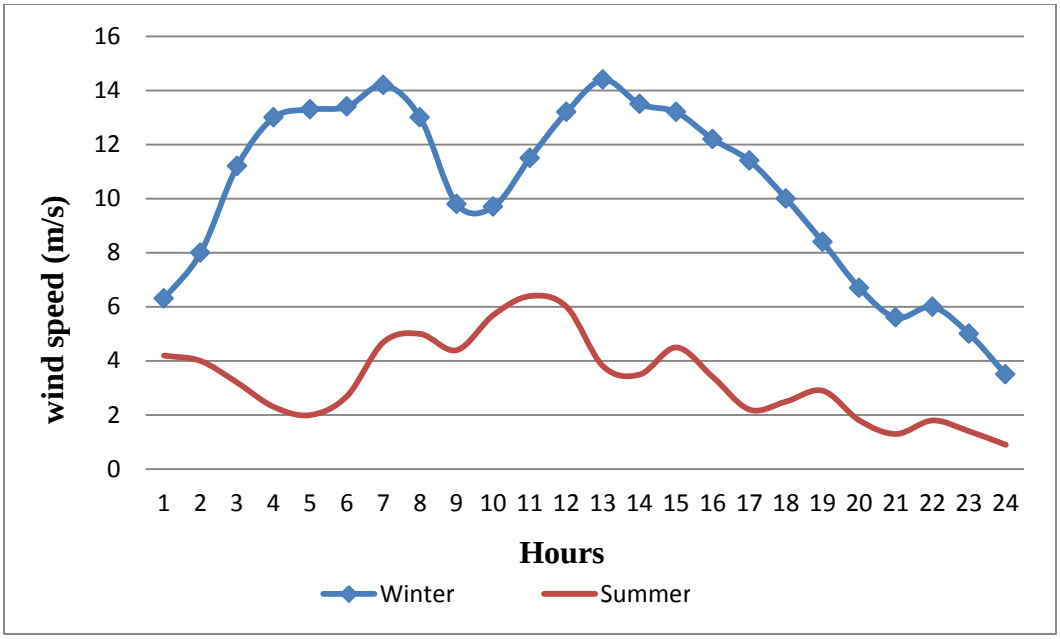

Figure 4-3: Wind speed profile for winter and summer

4.3.3 Solar Source

The solar radiation profile of Waterloo, Ontario, (43° 39' N, 80° 32' W) is obtained from the NASA Surface Meteorology and Solar Energy website [56]. The annual average solar radiation for this area is 3.64 kWh/m^2/day.

During winter season, Waterloo receives a typical low solar radiation profile, while it has high solar radiation during summer. Therefore, in this chapter two typical solar radiation profiles are examined, one for winter and the other for summer, as shown in Figure 4-4.

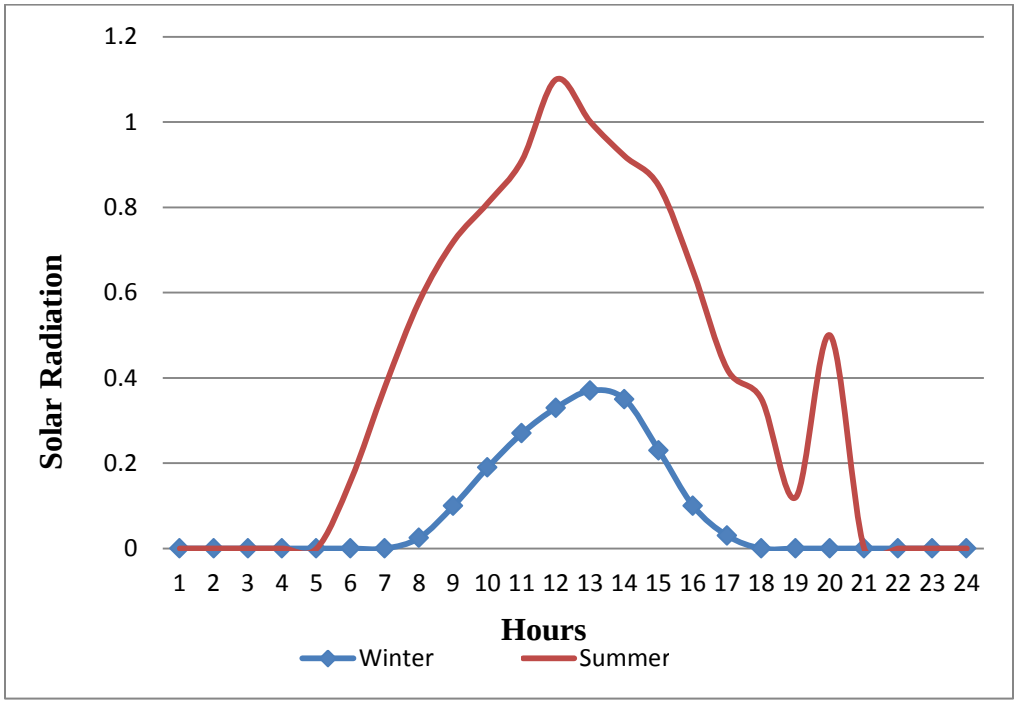

Figure 4-4: Solar radiation profiles for winter and summer (kWh/m^2)

4.4 Results and Discussions

In this chapter, the impact of coordinated operation of renewable energy sources and charging of PHEVs, on the distribution system performance is examined. Two scenarios, as in Chapter-3, are considered again here. Scenario 2 minimizes the total system losses, while Scenario 3 minimizes the PHEV charging cost to the customer, and hence the objective is to determine the optimal charging profile of PHEVs under different load conditions. Since renewable energy sources, such as wind and solar PV, are dependent on natural factors for example, temperature, humidity, wind speed and direction, two different seasons- winter and summer, are selected to find the effect of natural factors on the output of the renewable generation and thus the behaviour of system performance. The first season used is the winter season and the summer season is used as second season, these two season are selected because the wind and the solar PV output have a significant different in the selected site. After the proposed model is run the comparison between the results of different objectives with renewable energy contribution is conducting and discussed in this part.

The total system losses for different cases are presented in Table 4-1. From Table 4-1 it is observed that, the renewable energy sources significantly reduce the total system losses in both Scenarios 2 and 3, as compared with the case when there are no renewable energy sources (in chapter 3). For both scenarios 2 and 3, the most favorable charging cycle is during period 1, the overnight off-peak load. Comparing across the scenarios, it is noted that there is a significant saving in total system losses in Scenario 2 as compared to Scenario 3 in all periods. In Scenarios 2 and 3 during the winter season, which has high penetration of wind generation in the proposed site, the total system losses are lower as compared to the summer season for all periods.

Table 4-1: Total system losses (MW)

Period	Scenario 2: Minimum Loss		Scenario 3: Minimum Cost	
	Winter data	Summer data	Winter data	Summer data
	Winter TOU	Summer TOU	Winter TOU	Summer TOU
1	3.615	4.517	4.524	5.689
2	3.848	4.915	4.679	6.045
3	4.574	5.379	5.178	6.423

The wind generation profile as well as the solar PV generation in winter and summer seasons, using the proposed model, are presented in Figures 4-5 and 4-6 respectively.

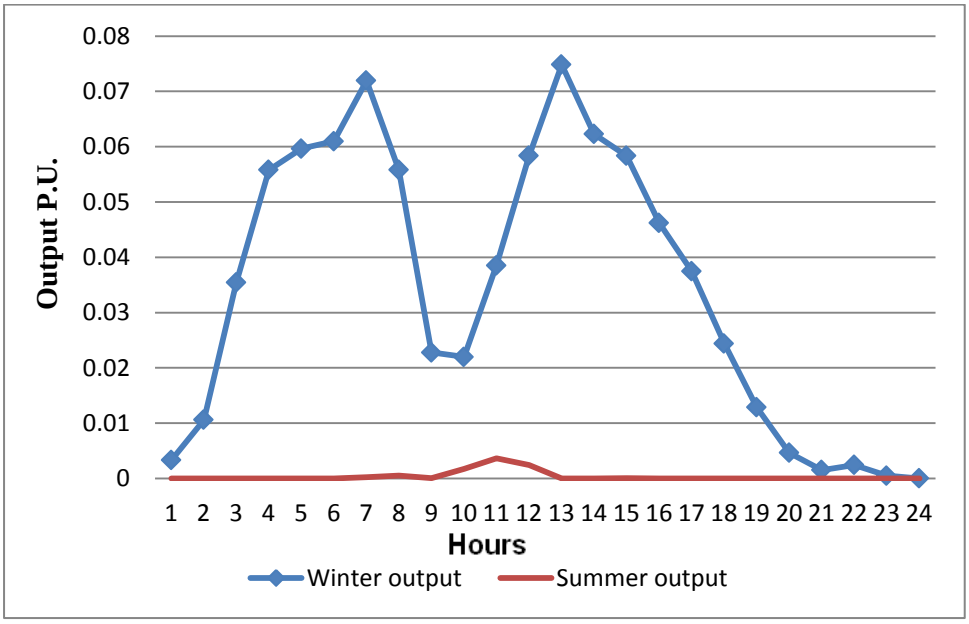

Figure 4-5: Wind generation profile

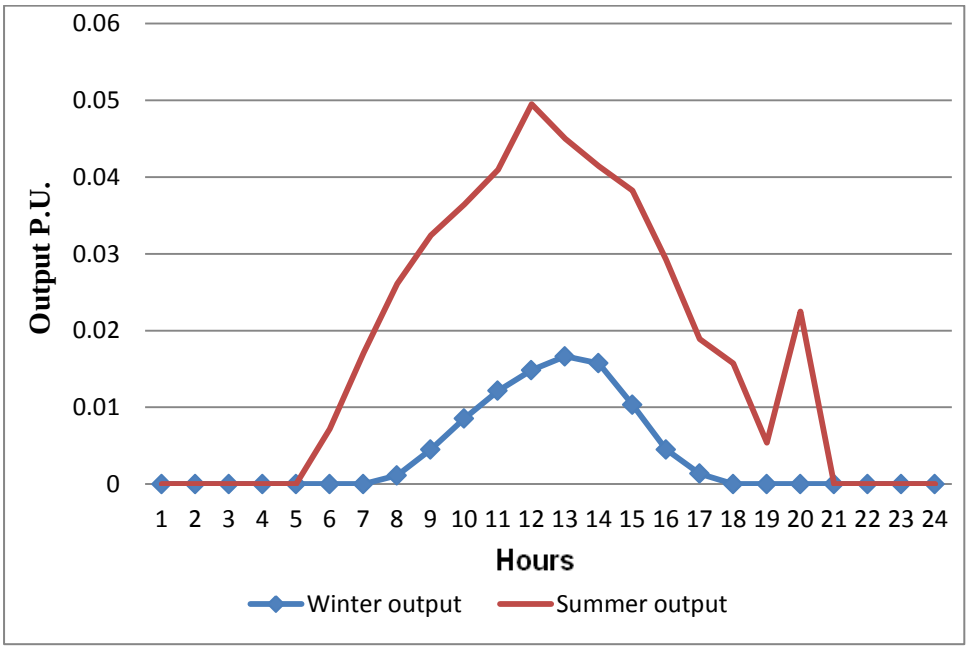

Figure 4-6: Solar generation profile

The charging decisions are obtained for each charging period, considered independent of each other, although the charging profiles presented in Figure 4-7, depict a 24-hour horizon.

As can be seen in Figure 4-7, the charging profile of the PHEVs in Scenario 2, is spread over all the charging periods almost uniformly, and there is no effect of TOU prices. However, there are some effects of varying renewable energy penetration, observed in the PHEV charging profile. The PHEV charging profile in Scenario 3 changes significantly from hour to hour depending on the TOU prices, and do not use the entire charging period to charge the battery, and hence results in rapid charging.

It is also noted that there are significant differences in the charging profiles obtained using the summer TOU rates and the winter rates, for period-2 and 3, when there are seasonal differences in the rates.

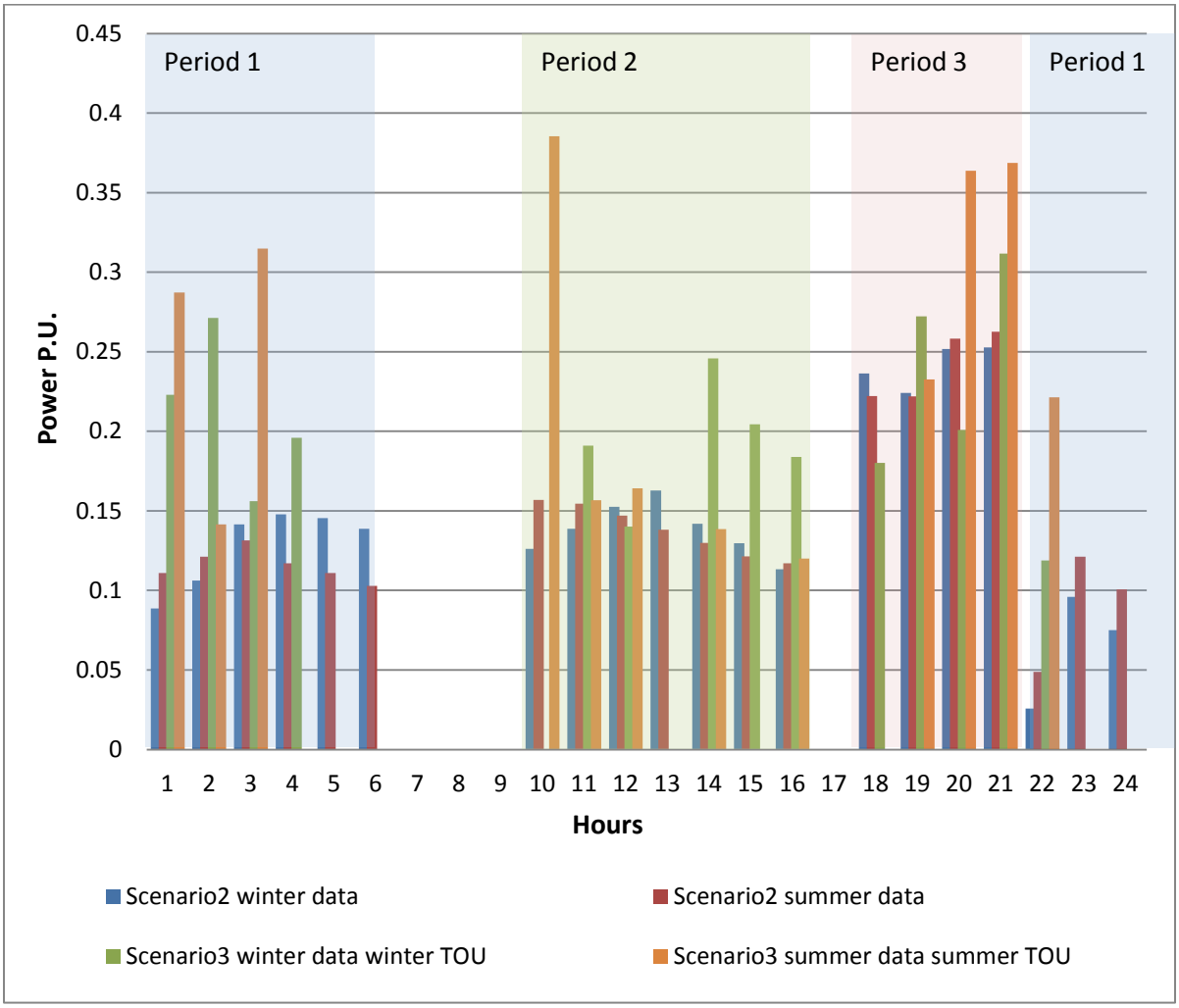

Figure 4-7: Optimal charging profile of PHEV in different scenarios

Table 4-2 presents a comparative summary of the total PHEV charging costs incurred in the two scenarios, for each charging period and both season of renewable energy data. As expected, Scenario 3 which minimizes the PHEV charging cost, results in minimum costs for periods 2 and 3 for both summer and winter TOU prices. However, there is no change in the PHEV charging cost during period 1, across the two scenarios because the TOU tariff is the same during the period.

Table 4-2: Total PHEV charging cost, $

Period	Scenario 2		Scenario 3	
	Winter data	Summer data	Winter data	Summer data
	winter TOU	summer TOU	winter TOU	summer TOU
1	569.35	569.35	569.35	569.35
2	881.54	1004.33	858.85	963.17
3	1032.55	636	1032.55	569.35

The Figures 4-8 to 4-10, present the voltage profiles at some specific buses for the charging periods to examine the impact of PHEV charging and renewable energy sources in various scenarios.

It is noted that PHEV charging in Scenario 2, for different seasons of renewable energy data, results in almost similar and high voltage profiles for both seasons. However, for those buses located near the PHEV charging station, for example bus-65, there is a significant change in the voltage profile. It is seen that PHEV charging in Scenario 3 during period 3 results in some voltage drop for both seasons and both TOU rates, but the voltage drop is significant if PHEV charging is in period 2. For example, bus-65 which is a remote bus and located near the PHEV charging station, is the one most affected, with its voltage being close to the lower allowable limit of 0.90 p.u. during period 2 and period 3.

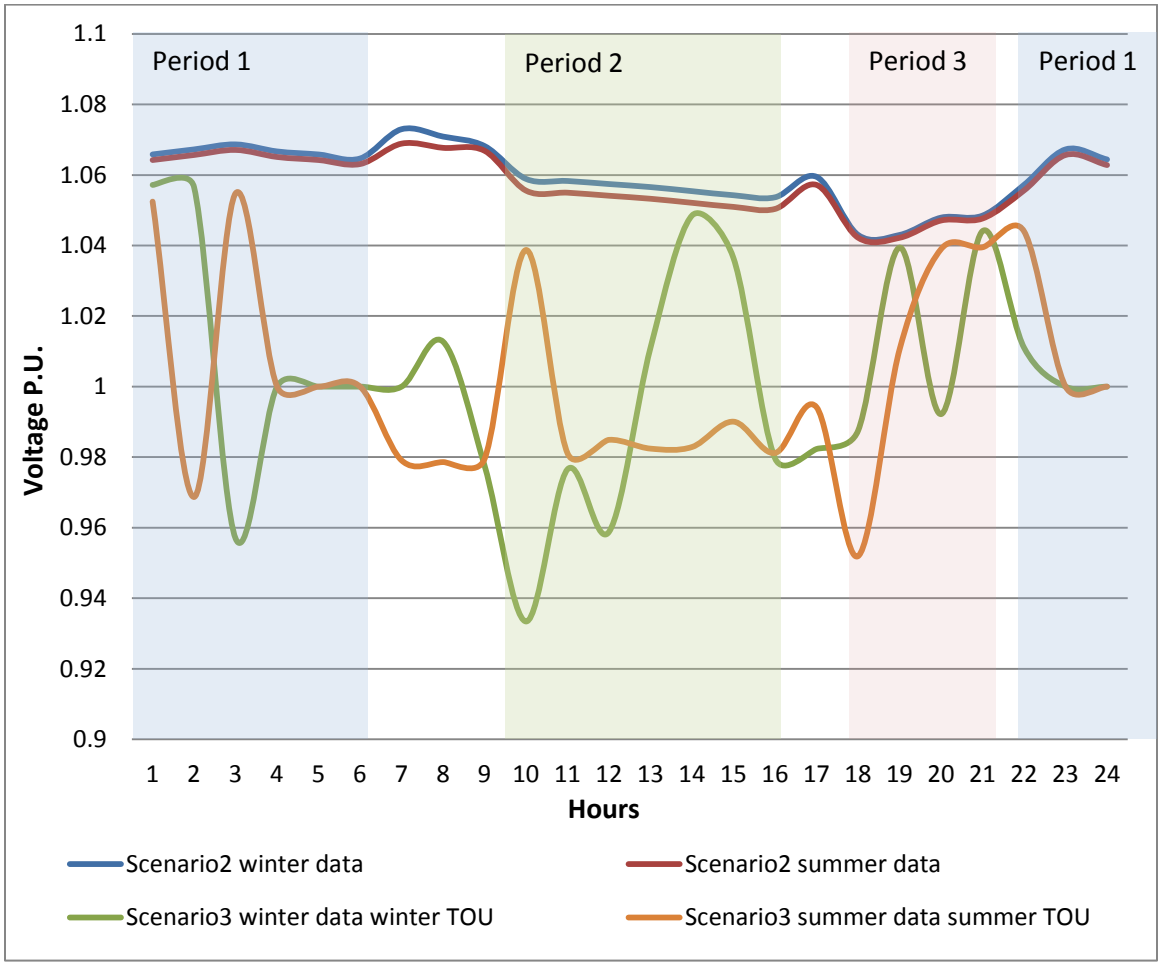

Figure 4-8: Voltage profile at bus 27

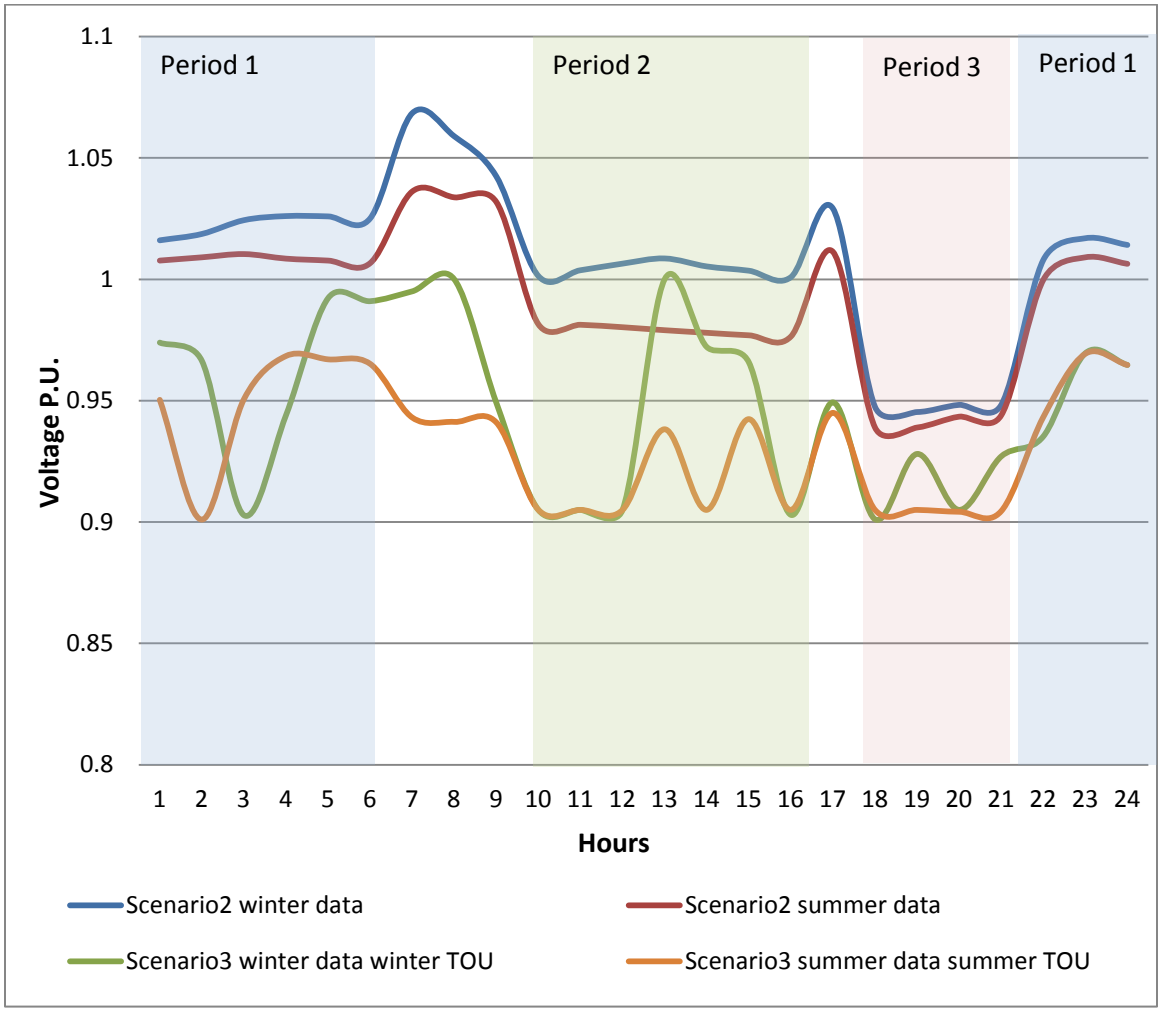

Figure 4-9: Voltage profile at bus 65

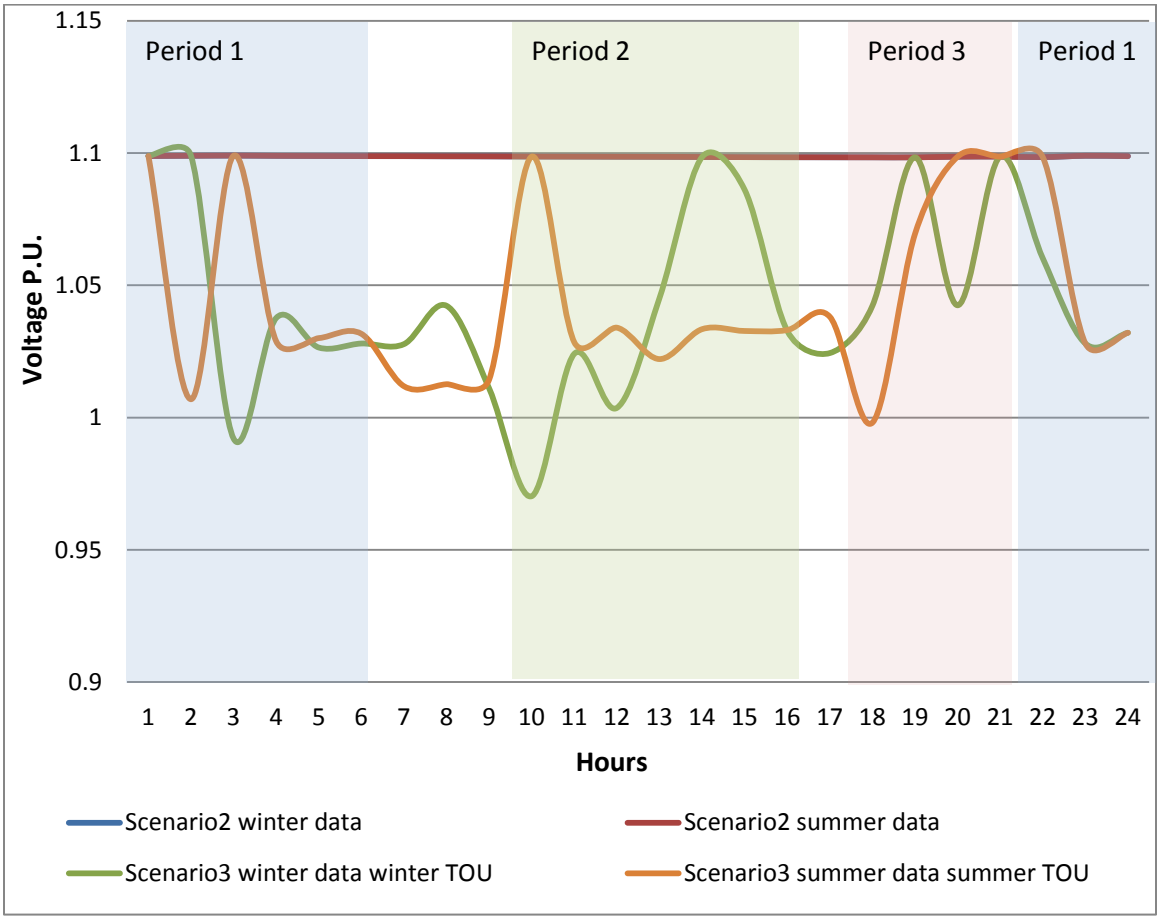

Figure 4-10: Voltage profile at bus 46

Figure 4-11 presents the active power transferred through the transformer for various scenarios. As expected, when the PHEV charging is taking place in Scenario 3 the active power transferred through the transformer increases for all periods as compared to Scenario 2. However, increase in the active power transfer through the transformer is significant if PHEV charging is considered in Scenario 3 and with summer data of renewable energy sources. It is noted that in Scenario 3 and summer TOU rate, the transformer operates close to its upper allowable limit in periods 2 and 3.

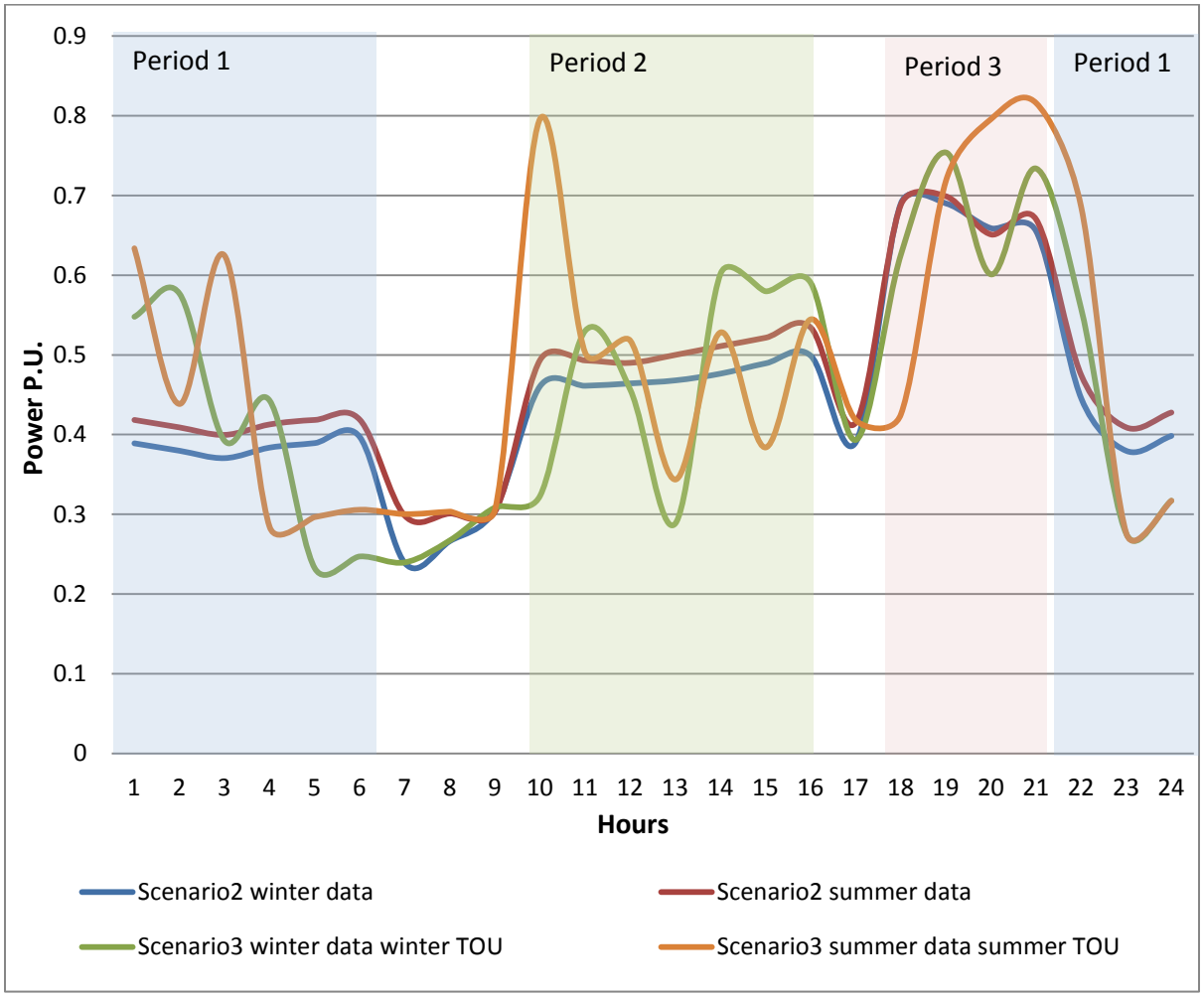

Figure 4-11: Active power transfer over substation transformer

The reactive power transferred through the transformer for various scenarios are presented in Figure 4-12. It can be observed that in Scenario 2, the reactive power transferred through the transformer for both seasons are almost equal. The reactive power transferred through the transformer is increased in Scenario 3 in comparison to the Scenario 2. It is noted that in Scenario 3 and summer TOU rate, the reactive power transferred through the transformer is increased even in periods 2 and 3.

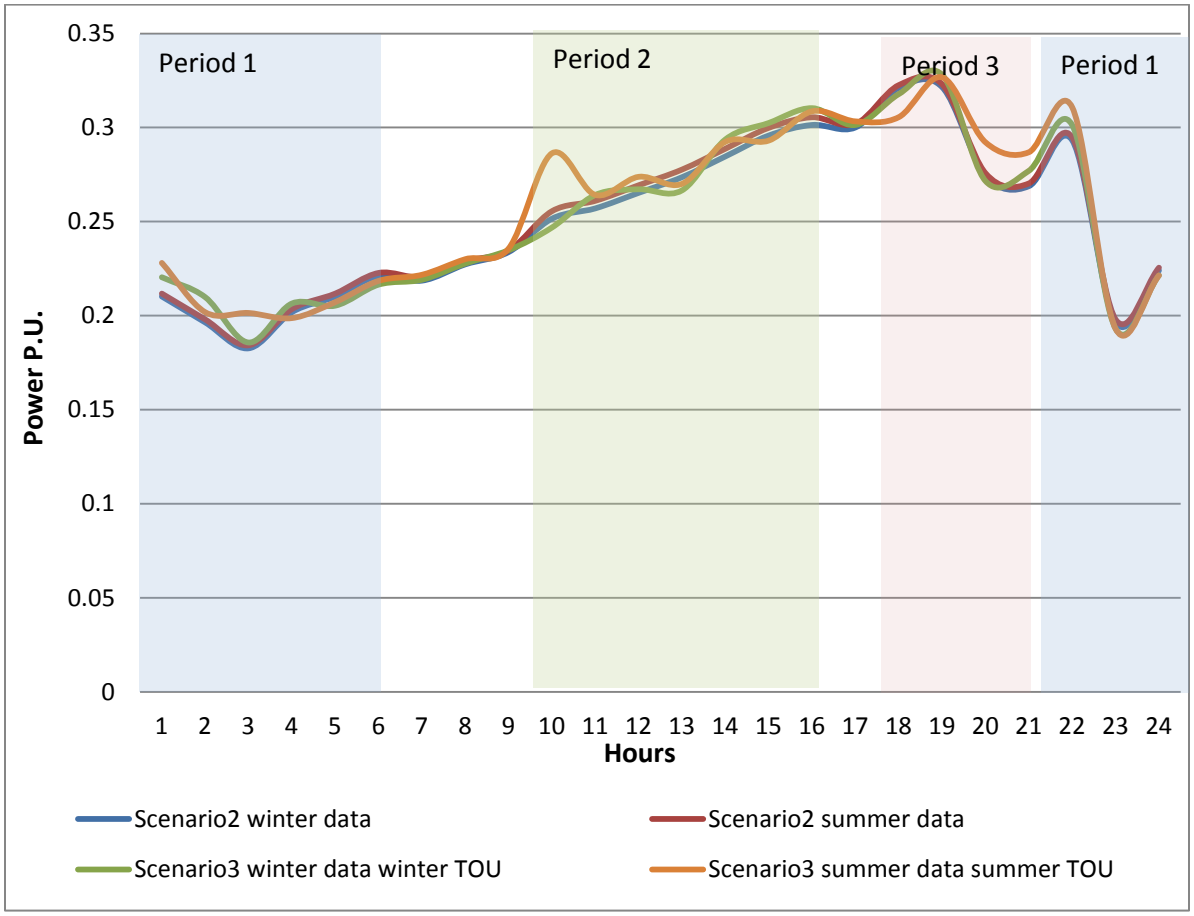

Figure 4-12: Reactive power transfer over substation transformer

4.5 Conclusions

The analysis presented in this chapter shows that the renewable energy sources are significantly critical in reducing the distribution system losses as well as the customers' cost. Moreover, renewable energy sources reduce the impact of charging PHEVs on the distribution system. In the selected site, the renewable energy sources have high output during winter season because of high output of wind generation during this period. Therefore, charging during period 1 and period 2 in the winter season are the most favorable periods because charging during these periods has the lower system losses and has reduction in the customer bill even though compared with the previous chapter results or other charging periods. However, charging during peak load time period 3 with taking into account the

renewable energy generation does not have that much of saving in the total system losses and in the customer bill compared with Base Case and other cases. In addition, the renewable energy output and their effect in the distribution during summer season is reduced because the selecting site has lower wind penetration during summer season and the solar PV output is not that much as ranking in high temperature countries. Finally, combined the renewable energy sources as well as PHEVs in the distribution system can significantly reduced the emission, losses of the system, and maximized the saving in the PHEV charging cost. Although, the renewable energy system playing significant role in the distribution system performance even if there is need to serve for extra load such as charging PHEVs.

Chapter 5

Summary and Conclusions

5.1 Summary of the Thesis

In this thesis, the optimal design and comparative studies for different microgrid configurations are discussed. Furthermore, the impacts of PHEV charging on the distribution system from the perspective of both the distribution utility and PHEV customers, are studied in details.

- Chapter 1 presents the motivation and background of the research problem and lays out the objectives of this thesis. In addition, a review of the literature on microgrids, renewable energy, and PHEV as well as smart charging is presented.
- Chapter 2 presents the optimal design and planning for four different cases of microgrid configurations including a diesel-only, a fully renewable-based, a diesel-renewable mixed, and an external-grid connected microgrid. The comparison and evaluation of their economics, operational performance and environmental emissions are discussed. Various renewable energy options such as solar PV, wind, micro-hydro and batteries are considered as possible options in the microgrid supply plan. Analysis is also carried out to determine the break-even grid extension distance from the microgrid location. Studies are carried out using the HOMER software which provides a very efficient tool for case studies and policy analysis.
- Chapter 3 presents an OPF based optimization framework considering two different objectives, minimizing feeder losses and PHEV charging cost, while meeting distribution system constraints to understand the impact of PHEV charging on distribution networks. Three different charging periods are considered and the impact of the TOU tariff on PHEV charging schedules is examined.
- Chapter 4 discusses the impact of PHEV charging on distribution systems in the presence of renewable energy sources. In order to determine the optimal charging

periods of PHEVs as well as the impact of renewable energy sources, the OPF based model developed in Chapter 3 is extended to include the contribution of renewable energy sources. The proposed model is evaluated under a variety of scenarios.

5.2 Main Conclusions and Contributions

The following are the main conclusions and contributions of the research presented in this thesis:

- The optimal design, planning, sizing and operation of a hybrid, renewable energy based microgrid with the goal of minimizing the lifecycle cost, while taking into account environmental emissions is presented in this thesis. Various renewable energy sources are considered as possible options in the microgrid supply plan. Analysis reveals that the diesel-renewable mixed microgrid has the lowest NPC and a fairly small carbon footprint, when compared to a stand-alone diesel-based microgrid. Although a fully renewable-based microgrid, which has no carbon footprint, is the most preferred, the NPC is higher. Also, the calculation of break-even distance, presented in this chapter, shows that for isolated microgrids, far away from the external grid connectivity point, the diesel-renewable mixed microgrid, is the optimal choice.
- An OPF model considering two different objectives, minimizing feeder losses and charging cost is applying to the 69-bus distribution system. The purpose of this study was to investigate an optimal operation strategy for a distribution system using GAMS simulation. From the results conducted it can be observed that, charging the PHEVs during period 1, is not significantly affected the daily operation of the proposed distribution system and it is the most favorable charging period because it has the minimum total system losses, as well as minimum cost in comparison to the others charging periods. The optimal charging profile is determined using the proposed model. Finally, the proposed optimal load flow model is found to be a very

helpful tool for examined the mentioned distribution system coupled with PHEVs charging impact.

- When the renewable energy sources are available as shown in Chapter 4 the proposed system becomes more reliable because from the results obtained, it can be clearly seen that the renewable energy sources are significantly reduced the distribution system losses as well as the customer bill cost. Charging during period 1 and period 2 in the winter season is the most favorable periods because on selected site the contribution renewable energy sources have high output during winter season. In addition, the renewable energy output and their effect during summer season is reduced because the selecting site has lower wind output during summer season and the solar PV penetration is not that much as ranking in high temperature countries. Finally, combined the renewable energy sources as well as PHEVs in the distribution system can significantly reduced the emission, losses of the system, and maximized the saving in the PHEV customer cost. Although, the renewable energy system playing significant role in the distribution system performance even if there is need to serve for extra load such as charging PHEVs.

5.3 Scope for Future Work

Based on the research presented in this thesis, some further research ideas and directions can be identified, as follows:

- The analysis could be carried out to examine the impact of PHEV charging environment, for example, the cost of CO_2 reduction be incorporated along with the renewable energy sources.
- A classical load flow optimization model could be developed considering the feeder thermal limit to determine the optimal capacity required of the distribution feeders. So that the existing plans could be modified based on the optimal sizing of PHEV charging station for the existing distribution system.

- In large scale distribution systems and in highly populated areas, there is a need to install multiple PHEV charging stations. Hence optimization techniques could be used to determine the optimal charging schedule for all the charging stations.
- This study could be extended to account for Level-1 PHEV charging which is a more popular outlet in Canada and USA.

References

[1] International Energy Agency, Key World Energy Statistics 2006. [Online]. Available: http://www.iea.org/

[2] World Energy Outlook. [Online]. Available: http://www.worldenergyoutlook.org/

[3] S. Rehman and L. Al-Hadhrami, "Study of a solar PV–diesel–battery hybrid power system for a remotely located population near Rafha, Saudi Arabia", Proceedings of 3rd International Conference on Sustainable Energy and Environmental Protection (SEEP 2009), Vol. 35, Issue 12, December 2010, Pages 4986 – 4995.

[4] Transport Canada. [Online]. Available: http://www.tc.gc.ca/environment/menu.htm#climatechange

[5] Ontario Power Authority, "Ontario's Integrated Power System Plan: Scope and Overview," June 2006 [online]. Available: http://www.powerauthority.on.ca/Storage/24/1922_OPA__IPSP_Scope_and_Overview.pdf

[6] M. Duvall and E. Knipping, "Environmental assessment of plug-in hybrid electric vehicles," Electric Power Research Institute (EPRI), 2007.

[7] T. S. Ustun, C. Ozansoy, A. Zayegh, "Recent developments in microgrids and example cases around the world—A review," Renewable and Sustainable Energy Reviews 15 (2011) 4030– 4041.

[8] N. Hatziargyriou., "MICROGRIDS – large scale integration of micro-generation to low voltage Grids,". [Online]. Available: http://microgrids.eu/micro2000/presentations/16.pdf.

[9] L. Robert, A. Abbas, M. Chris, S. John, D. Jeff, G. Ross, M. A. Sakis, Y. Robert, E. Joe "Integration of distributed energy resources: the CERTS MicroGrid concept ", Lawrence Berkeley National Laboratory ; 2002.

[10] N. Hatziargyriou "Microgrids", IEEE Power and Energy Magazine, 2007; vol.5: pp78–94.

[11] F. Z. Peng, Y. W. Li and L. M. Tolbert, "Control and protection of power electronics interfaced distributed generation systems in a customer-driven microgrid". In: Presented at IEEE the Power & Energy Society General Meeting, PES '09. 2009.

[12] Natural Resources Canada. [Online] Available: http://www.nrcan.gc.ca/eneene/renren/aboaprren-eng.php#what

[13] European Wind Energy Association (EWEA). Record growth for global wind power in 2002; 2002.

[14] Canadian Wind Energy Association. [Online] Available: www.canwea.ca.

[15] J. Ayoub, L. Dignard and A. Filion, "Photovoltaics for buildings: opportunities for Canada" CanmetENERGY , Natural Resources Canada. Dec 2001.

[16] Prof. T. Abdel-Galil, "Lecture Notes: ECE 667", Department of Electrical & Computer Engineering, University of Waterloo, Fall 2009.

[17] A comprehensive guide to plug-in hybrid vehicles, Hybrid Cars, [Online] Available: http://www.hybridcars.com/plug-in-hybrid-cars#battery, (2011).

[18] S. W. Hadley, "Impact of Plug-in Hybrid Vehicles on the Electric Grid", ORNL, [Online] Available: http://apps.ornl.gov/~pts/prod/pubs/ldoc3198_plug_in_paper_final.pdf, October, 2006

[19] M. Duvall, "Grid integration of plug-in hybrid and electric vehicles," in PHEV Executive Summit, Electric Power Research Institute (EPRI), July 2009.

[20] M. Ehsani, Y. Gao, S. E. Gay, A. Emadi "Modern Electric, Hybrid Electric, and Fuel Cell Vehicles Fundamentals, Theory, and Design" ISBN: 9781420054002

[21] C. Canizares, J. Nathwani, K. Bhattacharya, M. Fowler, M. Kazerani, R. Fraser, I. Rowlands, H. Gabbar, "Towards an Ontario Action Plan For Plug-In-Electric Vehicles (PEVs)" Waterloo Institute for Sustainable Energy, University of Waterloo, May 17, 2010.

[22] Vehicle-Grid Interface Key to Smart Charging Plug-in Vehicles [Online] Available: http://www.transportation.anl.gov/pdfs/HV/617.PDF

[23] A. Kornelakis and Y. Marinakis, “Contribution for optimal sizing of grid-connected PV-systems using PSO”, Renewable Energy, Vol.35, 2010, 1333–1341.

[24] C. Nayar, M. Tang and W. Suponthana, “Wind / PV / Diesel microgrid system implemented in remote islands in the Republic of Maldives”, Proceeding of IEEE International Conference on Sustainable Energy Technologies 2008 (ICSET), Nov. 2008, pp.1076 - 1080.

[25] D. Thiam, “Renewable decentralized in developing countries: Appraisal from microgrids project in Senegal”, Renewable Energy Vol.35, 2010, 1615–1623.

[26] M. Anyi, B. Kirke and S. Ali, “Remote community electrification in Sarawak, Malaysia”, Renewable Energy Vol.35, 2010, 1609–1613.

[27] J. Kaldellis, “Optimum hybrid photovoltaic-based solution for remote telecommunication stations”, Renewable Energy Vol.35, 2010, 2307-2315.

[28] Z. Muis, H. Hashim, Z. Manan, F. Taha and P. Douglas, “Optimal planning of renewable energy-integrated electricity generation schemes with CO_2 reduction target”, Renewable Energy Vol.35, 2010, 2562 – 2570.

[29] S. Mizani and A. Yazdani, “Optimal design and operation of a grid-connected microgrid”, Proceedings of IEEE Electrical Power & Energy Conference, 2009.

[30] HOMER analysis https://analysis.nrel.gov/homer/

[31] A. Prasai, A. Paquette, Y. Du, R. Harley and D. Divan, “Minimizing emissions in microgrids while meeting reliability and power quality objectives”, Proceeding of 2010 International Power Electronics Conference.

[32] D. Lee, J. Park, H. Shin, Y. Choi, H. Lee and J. Choi, “Microgrid village design with renewable energy resources and its economic feasibility evaluation”, Proceeding of IEEE T&D Asia 2009.

[33] W. Gu, Z. Wu and X. Yuan, “Microgrid economic optimal operation of the combined heat and power system with renewable energy”, Proceeding of Power and Energy Society General Meeting, 2010 IEE, pp. 1 - 6.

[34] S. Chakraborty and M. Simoes, "PV-Microgrid operational cost minimization by neural forecasting and heuristic optimization," Proceeding of Proc. IEEE-IAS Annual Meeting, Oct. 2008, pp. 1-8.

[35] A. Kanase-Patil, R. Saini and M. Sharma, "Integrated renewable energy systems for off grid rural electrification of remote area", Renewable Energy Vol.35, 2010, 1342–1349.

[36] B. Kroposki and G. Martin, "Hybrid renewable energy and microgrid research work at NREL", Proceeding of Power and Energy Society General Meeting, 2010 IEEE, 25-29 July 2010, ISSN: 1944-9925.

[37] P. Díaz, C.A. Arias, R. Peña and D. Sandoval, "FAR from the grid: A rural electrification field study", Renewable Energy Vol.35, 2010, pp. 2829-2834.

[38] I. Mitra, T. Degner and M. Braun, "Distributed generation and microgrids for small island electrification in developing countries", SESI JOURNAL, 2008 Solar Energy Society of India Vol. 18 No. 1 January-June 2008, pp. 6-20.

[39] G. T. Heydt, "The impact of electric vehicle deployment on load managment strategies," IEEE Transactions on Power Apparatus and Systems, vol. 1, no. 144, pp. 1253–1259, 1983.

[40] A. Heider and H. J. Haubrich, "Impact of wide-scale EV charging on the power suppy network," IEE Colloqium on Electric Vehicles – A technology roadmap for the future, vol. 6, no. 262, pp. 1–4, 1998.

[41] K. Schneider, C. Gerkensmeyer, M. Kintner-Meyer, and M. Fletcher, "Impact assessment of plug-in hybrid electric vehicles on pacific northwest distribution systems," IEEE Power and Energy Society 2008General Meeting, Pittsburgh, Pennsylvania USA, 2008.

[42] W. Kempton and J. Tomic, "Vehicle-to-grid power fundamentals: Calculating capacity and net revenue," Journal of Power Sources, vol. 144, pp. 280–294, 2005.

[43] C. Roe, F. Evangelos, J. Meisel, S. Meliopoulos and T.Overbye, "Power system level impacts of PHEVs", in Proc. 42nd Hawaii Int. Conf. Syst. Sci., 2009, pp. 1-1.

[44] J. A. P. Lopes, P. M. R. Almeida, and A. M. M. da Silva, ”Smart charging strategies for electric vehicles: Enhancing grid performance and maximizing the use of variable renewable energy sources”, in Proc. 24th Int. Battery Hybrid Fuel Cell Electr. Vehicle Symp. Exhib., Stavanger, Norway, May 2009, pp. 1-11.

[45] J. A. P. Lopes, F. J. Soares and P. M. R. Almeida, ”Integration of electric vehicles in the electric power system”, Proceedings of the IEEE, vol. 99, No. 1, 2011, pp. 168-183.

[46] K. Clement-Nyns, E. Haesen, and J. Driesen, “The impact of charging plug-in hybrid electric vehicles on a residential distribution grid,” IEEE Trans. Power Syst., vol. 25, no. 1, pp. 371–380, 2010.

[47] L. Kelly, A. Rowe, and P.Wild, “Analyzing the impacts of plug-in electric vehicles on distribution networks in British Columbia,” in Proc. IEEE Elect. Power Energy Conf., 2009, pp. 1–6.

[48] K. Clement, E. Haesen, and J. Driesen, “Coordinated charging of multiple plug-in hybrid electric vehicles in residential distribution grids,” in Proc. Power Syst. Conf. Expo., 2009, pp. 1–7.

[49] A. Hajimiragha, C. A. Cañizares,M.W. Fowler, and A. Elkamel, “Optimal transition to plug-in hybrid electric vehicles in Ontario, Canada, considering the electricity-grid limitations,” IEEE Trans. Ind. Electron., vol. 57, no. 2, pp. 690–701, Feb. 2010.

[50] C. H. Stephan and J. Sullivan, ”Environmental and Energy Implications of Plug-In Hybrid-Electric Vehicles,” Environ. Sci. Technol., 42, 11851190, 2008.

[51] V. Marano and G. Rizzoni, “Energy and Economic Evaluation of PHEVs and their Interaction with Renewable Energy Sources and the Power Grid”, in: Proc. IEEE International Conference on Vehicular Electronics and Safety, 2008.

[52] X. Li, L. A. C. Lopes, and S. S. Williamson, “On the suitability of plug in hybrid electric vehicle (PHEV) charging infrastructures based on wind and solar energy”, in: Proc. IEEE Power & Energy Society General Meeting, PES 2009.

[53] S. Shao, T. Zhang, M. Pipattanasomporn and S. Rahman, ”Impact of TOU rates on distribution load shapes in a smart grid with PHEV penetration”, Transmission and Distribution Conference and Exposition, 2010, pp. 1-6.

[54] S. Rehman and L. Al-Hadhrami, "Study of a solar PV–diesel–battery hybrid power system for a remotely located population near Rafha, Saudi Arabia", Proceedings of 3rd International Conference on Sustainable Energy and Environmental Protection (SEEP 2009), Vol. 35, Issue 12, December 2010, Pages 4986 – 4995.

[55] T. Lambert, P. Gilman and P. Lilienthal, "Integration of Alternative Sources of Energy, chapter 15: Micropower system modeling with HOMER", National Renewable Energy Laboratory, 5 APR 2006.

[56] NASA Surface Meteorology and Solar Energy. [Online] available: http://eosweb.larc.nasa.gov/sse/.

[57] Canadian wind energy atlas. [Online] available: http://www.windatlas.ca/en/nav.php.

[58] Ontario Hydro Rates. [Online] available: http://www.ontario-hydro.com/index.php?page=current_rates

[59] A. Algarni, "Operational and Planning Aspects of Distribution Systems in Deregulated Electricity Markets", Ph.D Thesis, University of Waterloo, 2009.

[60] N. D. Hatziargyriou, T. S. Karakatsanis, and M. Papadopoulos, "Probabilistic load flow in distribution systems containing dispersed wind power generation," *IEEE Trans. Power Syst.*, vol. 8, no. 1, pp. 159–165, Feb. 1993.